ผลของรูปร่างสารฝังในต่อการตอบสนองทางไฟฟ้าของไดอิเล็กทริกคอมพอสิตไม่เชิงเส้น

นายจตุพร ทองศรี

วิทยานิพนธ์นี้เป็นส่วนหนึ่งของการศึกษาตามหลักสูตรปริญญาวิทยาศาสตรดุษฎีบัณฑิต
สาขาวิชาฟิสิกส์ ภาควิชาฟิสิกส์
คณะวิทยาศาตร์ จุฬาลงกรณ์มหาวิทยาลัย
ปีการศึกษา 2553

EFFECTS OF INCLUSION SHAPES ON ELECTRIC RESPONSES OF NONLINEAR DIELECTRIC COMPOSITES

Mr. Jatuporn Thongsri

A Dissertation Submitted in Partial Fulfillment of the Requirements
for the Degree of Doctor of Philosophy Program in Physics
Department of Physics
Faculty of Science
Chulalongkorn University
Academic Year 2010

Thesis Title	EFFECTS OF INCLUSION SHAPES ON ELECTRIC RESPONSES OF NONLINEAR DIELECTRIC COMPOSITES
By	Mr. Jatuporn Thongsri
Field of Study	Physics
Thesis Advisor	Associate Professor Mayuree Natenapit, Ph.D.

Accepted by the Faculty of Science, Chulalongkorn University in Partial Fulfillment of the Requirements for the Doctoral Degree

S. Hannongbua ..... Dean of the Faculty of Science

(Professor Supot Hannongbua, Dr.rer.nat)

THESIS COMMITTEE

Patcha Chatraphorn ..... Chairman

(Assistant Professor Patcha Chatraphorn, Ph.D.)

Mayuree Natenapit ..... Thesis Advisor

(Associate Professor Mayuree Natenapit, Ph.D.)

V. Hengpunya ..... Examiner

(Varagorn Hengpunya, Ph.D.)

Orapin Wannadelok ..... Examiner

(Orapin Wannadelok, Ph.D.)

..... External Examiner

(Assistant Professor Sutee Boonchui, Ph.D.)

จตุพร ทองศรี : ผลของรูปร่างสารฝังในต่อการตอบสนองทางไฟฟ้าของไดอิเล็กทริกคอมพอสิตไม่เชิงเส้น (EFFECTS OF INCLUSION SHAPES ON ELECTRIC RESPONSES OF NONLINEAR DIELECTRIC COMPOSITES) อ. ที่ปรึกษาวิทยานิพนธ์หลัก : รศ.ดร.มยุรี เนตรนภิส, 74 หน้า.

ได้ศึกษาผลการตอบสนองทางไฟฟ้าของไดอิเล็กทริกคอมพอสิตไม่เชิงเส้นสองชนิด ได้แก่ชนิดที่สารฝังในมีลักษณะรูปร่างเหมือนกันกับอีกชนิดที่สารฝังในมีการกระจายของลักษณะรูปร่าง โดยสารฝังในกระจายแบบสุ่มอยู่ในตัวกลางเชิงเส้นอย่างเบาบาง มีสมบัติไดอิเล็กทริกความสัมพันธ์ระหว่างการกระจัดทางไฟฟ้า $(\boldsymbol{D})$ และสนามไฟฟ้าของสารฝังในคือ $\boldsymbol{D} = \varepsilon \boldsymbol{E} + \chi |\boldsymbol{E}|^{\beta} \boldsymbol{E}$ เมื่อ β คือ เลขจำนวนเต็มชี้กำลังความไม่เชิงเส้น และ $\varepsilon \gg \chi |\boldsymbol{E}|^{\beta}$ สำหรับคอมพอสิตไม่เชิงเส้นอย่างอ่อน สำหรับคอมพอสิตไม่เชิงเส้นอย่างแรง สมบัติไดอิเล็กทริก $\boldsymbol{D} = \chi |\boldsymbol{E}|^2 \boldsymbol{E}$ ถูกพิจารณาทั้งในสารฝังในและในตัวกลาง โดยการใช้วิธีการประมาณแบบแยก สัมประสิทธิ์ไม่เชิงเส้นยังผล (χ_e) ได้ถูกคำนวณและรายงานในเทอมของค่าอัตราส่วนรูปร่าง (M) และค่าการกระจายลักษณะรูปร่าง (Δ) สำหรับคอมพอสิตชนิดแรกและชนิดหลังตามลำดับ สำหรับคอมพอสิตไม่เชิงเส้นอย่างอ่อนซึ่งสารฝังในมีลักษณะรูปร่างเหมือนกัน ผลการคำนวณแสดงให้เห็นการเพิ่มขึ้นอย่างรวดเร็วของค่า χ_e ตามการเพิ่มขึ้นของค่า M ในช่วงที่ M มีค่าต่ำ อย่างไรก็ตาม ในช่วงที่ M มีค่าสูง การเพิ่มขึ้นของค่า M มีผลต่อการเพิ่มขึ้นของค่า χ_e เพียงเล็กน้อย ลักษณะนี้ยังพบได้ในคอมพอสิตไม่เชิงเส้นอย่างแรงด้วย สำหรับคอมพอสิตซึ่งสารฝังในมีการกระจายของลักษณะรูปร่าง ผลการคำนวณแสดงการเพิ่มขึ้นหรือลดลงอย่างรวดเร็วของค่า χ_e เมื่อเพิ่มค่า Δ เฉพาะเมื่อ Δ มีค่าเข้าใกล้ 1 นอกจากนี้เรายังได้คำนวณค่า χ_e เชิงวิเคราะห์ที่แม่นตรงสำหรับคอมพอสิตไม่เชิงเส้นอย่างอ่อนในกรณี $\beta = 2$ อีกด้วย ซึ่งผลการคำนวณเชิงวิเคราะห์สอดคล้องกับผลการคำนวณเชิงตัวเลข

ภาควิชา.....ฟิสิกส์..... ลายมือชื่อนิสิต.....จตุพร ทองศรี.....

สาขาวิชา.... ฟิสิกส์..... ลายมือชื่อ อ.ที่ปรึกษาวิทยานิพนธ์หลัก.....

ปีการศึกษา.. 2553.....

4973808823 : MAJOR PHYSICS
KEYWORDS : DECOUPLING APPROXIMATION / ELLIPTICAL DIELECTRIC INCLUSIONS / NONLINEAR COMPOSITES

JATUPORN THONGSRI : EFFECTS OF INCLUSION SHAPES ON ELECTRIC RESPONSES OF NONLINEAR DIELECTRIC COMPOSITES. ADVISOR : ASSOC. PROF. MAYUREE NATENAPIT, Ph.D., 74 pp.

The electric field responses of two types of nonlinear dielectric composites consisting of elliptic cylindrical inclusions, one with an identical shape and another with distributed shapes, randomly embedded in the host media in the dilute limit are investigated. The dielectric property of the inclusions is that the relation between the displacement field ($\mathbf{D}$) and electric field ($\mathbf{E}$) satisfies a more general form $\mathbf{D} = \varepsilon\mathbf{E} + \chi|\mathbf{E}|^{\beta}\mathbf{E}$, where β is a nonlinear integer exponent and $\varepsilon \gg \chi|\mathbf{E}|^{\beta}$ for weakly nonlinear composites. For strongly nonlinear composites, the dielectric property of both inclusion and medium satisfying $\mathbf{D} = \chi|\mathbf{E}|^{2}\mathbf{E}$ is considered. By using the simple decoupling approximation, the effective nonlinear coefficients (χ_e) are determined and the effects of inclusion shapes on χ_e are reported in terms of the aspect ratio (M), and the shape distribution parameter (Δ) for the former and the latter types of composites, respectively. For weakly nonlinear composites with identical inclusion shape, the results show the rapid increase in χ_e with increasing M within the range of lower values of M. However, within the range of higher values of M, increasing M affects the increasing of χ_e very slightly. The similar behavior is also observed for strongly nonlinear composites. For composites with distributed inclusion shapes, the results reveal the rapid increase or decrease in χ_e with increasing Δ, especially, when Δ near 1. Furthermore, the exact analytic result of χ_e for weakly nonlinear elliptical composites with distributed inclusion shapes for the case of $\beta = 2$ is also determined and this is consistent with the numerical result.

Department : .....Physics.....
Field of Study : .....Physics.....
Academic Year : .....2010.....

Student's Signature ...Jatuporn Thongsri...
Advisor's Signature ...Mayuree Natenapit...

Acknowledgements

I would like to express my sincere thank and deep appreciation to my advisor, Assoc. Prof. Dr. Mayuree Natenapit for her excellent instructions, critical comments, guidance, suggestions and support throughout this thesis work. Special thanks also are extended to Asst. Prof. Dr. Patcha Chatraphorn, Dr. Varagorn Hengpunya, Dr. Orapin Wannadelok and Asst. Prof. Dr. Sutee Boonchui for teaching as thesis committee and for valuable comments.

Sincere thanks are extended to all friends of the Department of Physics for their suggestions, assistance and friendship.

The author would like to thank the Development and Promotion of Science and Technology Talent Project (DPST) for a scholarship support to this graduate study. The financial support of this work by the 90^{th} Anniversary of Chulalongkorn University Fund (Ratchadaphiseksomphot Endowment Fund) is gratefully acknowledged.

Finally, the greatest gratitude is expressed to my mother and my family for their love and understanding.

Contents

Chapter **Page**

Chapter **Page**

List of Figures

Figure **Page**

Figure **Page**

Figure **Page**

List of Symbols

ε_e	effective linear coefficient of composite
ε_i	effective linear coefficient of inclusion
ε_m	effective linear coefficient of medium
ε_r	linear contrast or relative linear coefficient ($\varepsilon_i/\varepsilon_m$)
χ_e	effective nonlinear coefficient of composite
χ_i	nonlinear coefficient of inclusion
χ_m	nonlinear coefficient of host medium
χ_r	nonlinear contrast or relative nonlinear coefficient (χ_i/χ_m)
v_i	inclusion packing fraction (volume fraction)
ϕ	electric potential
$\mathbf{E}_i$	electric field inside elliptic cylindrical inclusion
$\mathbf{E}_m$	electric field inside medium
$\mathbf{D}$	electric displacement
M	aspect ratio, the ratio between semi major and minor axes of elliptic cylindrical inclusion
α	an angle between the external electric field and the axis of the inclusion
β	nonlinear integer exponent
$\langle E_i^n \rangle$	volume average of electric field inside inclusion to the n^{th} power
L	depolarization factor
β_j	field factor in the direction j
$P(L)$	shape distribution function
Δ	shape distribution parameter

CHAPTER I

Introduction

The physics of nonlinear response of composites subject to an applied electric field has been very much interested because it has many applications in physics and engineering, for instance, developing photonic devices, explaining some physical phenomena, predicting optical responses and using as fundamental information for designing nonlinear optical materials [1]. For example, the color of laser light depends on the optical nonlinear response of material used in laser. If we can control the optical nonlinear response then we can control the color of the emitted laser light. Therefore, it is useful to study the electric field responses of these materials. Various methods have been used to study the effective responses of nonlinear composites such as the perturbation method [2-4], the variational method [5-8] and the decoupling approximation [9-12]. The decoupling approximation, originally proposed by Stroud and Wood [13], has been widely applied to study nonlinear composites by many authors [9 -12]. We previously have applied this method together with the variational method to predict the effective third-order nonlinear coefficient (χ_e) of strongly nonlinear spherical dielectric composites [14], and confirmed the results with the experimental data of Gehr et al. [15].

Obviously, the effective response depends on composite microstructures such as inclusion packing fraction and inclusion shapes. In the literature search, constituents of spherical and cylindrical geometries have been mostly presented for theoretical models in investigations of effective responses of composites. However, in experimental lab, the realistic constituents of prepared composites may not be perfectly spherical or cylindrical such as those of Kochergin et al.[16] and Piredda et al.[17] with imperfectly spherical and cylindrical nanoinclusions, randomly distributed in dielectric medium. Therefore, the research interests have been devoted

to the elliptical and ellipsoidal composites and also concentrated on the effect of inclusion shapes on nonlinear response.

To obtain the effective nonlinear responses very close to those of realistic composites, we consider the composite microstructures of two types, composites with identical inclusion shape and those with distributed inclusion shapes. For the former, the geometry of all inclusions is the same. For the latter, the inclusion shapes could deviate from a specific geometry such as cylinder to any possible shape of elliptic cylinders. For both cases, the inclusions are randomly embedded in the host medium with parallel axes.

For composites with identical inclusion shape, Hui and Chung [11] studied the effective nonlinear response in random composites consisting of weakly nonlinear cylindrical (and spherical) inclusions randomly embedded in the host medium. By using the effective medium approximation, the expression of effective nonlinear coefficient (χ_e) was derived. Giordano et al. [18-19] developed alternative procedure to investigate the shape-dependent effects of linear or nonlinear ellipsoidal dielectric inclusions randomly oriented and embedded in linear dielectric medium in terms of the eccentricity of the inclusions. Chang et al. [20] have investigated the effect of host medium and particle shapes on third-order optical nonlinearities of nanocomposites which compose of ZnO nanorods or ZnO nanoparticles suspended in water or ethanol. Their results are in good agreement with the theoretical predictions based on Maxwell-Garnett effective medium theory. Recently, we have applied the decoupling approximation to investigate the shape effect of identical inclusions on the effective nonlinear response of strongly nonlinear elliptical dielectric composites in the dilute limit [21]. We expect that composite microstructures of these work relate to those of Kochergin's experiment.

For composites with distributed inclusion shapes, based on statistical approach, Goncharenko et al. [22-23] successfully predicted the effect of shape distribution on light absorption and light scattering of ellipsoidal composites and their approach has been widely applied to study the electric field response by many authors [24-31]. The effective linear and nonlinear optical properties of metal-dielectric composites with inclusion shape distribution [24-26] have been in-

vestigated including the effective nonlinear response of a two-dimensional strongly nonlinear elliptic cylindrical composite by the effective medium approximation [27] and that of nonlinear ellipsoidal composite by Maxwell-Garnet approximation [28]. Xu and Li proposed that the particle shape has a profound effect on the optical threshold of metal-insulator composites [29]. Goncharenko et al. have predicted the shape distribution effect of nonsphericity on linear and nonlinear optical properties of small particles composites [30] and evaluated the effective dielectric response of core-shell particle of linear [31] and nonlinear composites [32]. We expect that the composite microstructures of these work relate to those of Piredda's experiment.

Further investigation and analysis of the effects of inclusion shapes on effective nonlinear responses for the two-dimensional nonlinear elliptical dielectric composites are presented in this research. The work of Hui and Chung [11] is extended to weakly and strongly nonlinear elliptic cylindrical composites with identical and distributed inclusion shapes. In Chapter 2, the brief details of the dielectric properties, the basic equations are reported. In Chapter 3, we consider the composites with identical inclusion shape. The dielectric property of the inclusions is that the electric displacement ($\mathbf{D}$) and electric field ($\mathbf{E}$) satisfies a more general relation $\mathbf{D} = \varepsilon\mathbf{E} + \chi|\mathbf{E}|^{\beta}\mathbf{E}$ where β is a nonlinear integer exponent. For weakly nonlinear composites $\varepsilon \gg \chi|\mathbf{E}|^{\beta}$ and $\varepsilon \ll \chi|\mathbf{E}|^{2}$ for strongly nonlinear composites are considered. By using the decoupling approximation, the effective nonlinear coefficients (χ_e) are determined, and then the effects of inclusion shapes on χ_e are reported for varying the aspect ratios (the ratios between the semi-major and semi-minor axes for identical inclusions). In Chapter 4, we focus on the composites with distributed inclusion shapes having the same dielectric property as composites with identical inclusion shape. Based on the statistical approach and the decoupling approximation, χ_e and the effects of inclusion shapes on χ_e are reported for varying the shape distribution parameter. Finally, discussion and conclusions of our theoretical results are given in the last section.

CHAPTER II

Theoretical Background

In this chapter, the brief details of the dielectric properties and the basic equations of composites subject to an external electric field will be reported. These play important roles in investigation of the electric field responses of dielectric composites in Chapters 3 and 4.

2.1 Dielectric Media

2.1.1 Polarization (P)

In general, the molecules are classified into two types: polar and nonpolar molecules. In a polar molecule, the center of the electric charge is permanently displaced from the center of the nucleus charge so the neutral molecule has a permanent electric dipole moment. The water molecule is an example of polar molecule. In contrast, if the centers of positive and negative charges are not displaced relative to each other, then the molecule does not exhibit a permanent electric dipole (nonpolar molecule). Examples of nonpolar molecules include O_2, N_2, and H_2.

Now, we consider the interaction between individual molecules (or atoms) and the electric field. If the atom is neutral and unpolarized, the dipole moment is zero as in Figure 2.1. When an external electric field is applied, the electron cloud becomes slightly displaced or asymmetrical, as in Figure 2.2, and the atom is polarized having a tiny dipole moment $\mathbf{p}$, which points in the same direction as the electric field. For polar molecules (or atoms), the external electric field

rotates the dipole moments to the direction of the external electric field. Figure 2.3 shows the polar molecules of water in an electric field. The electric field creates the polarization (**P**) which is the dipole moment per unit volume.

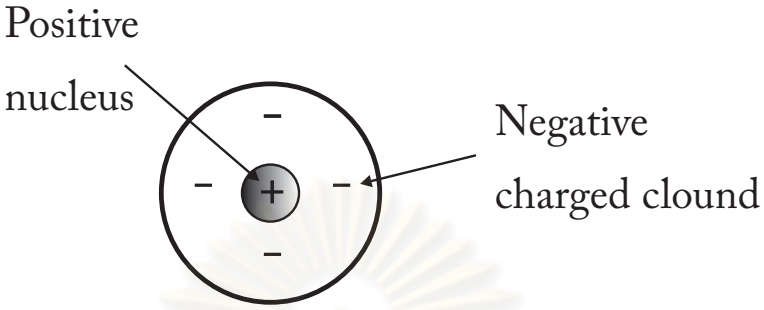

Figure 2.1: An unpolarized atom.

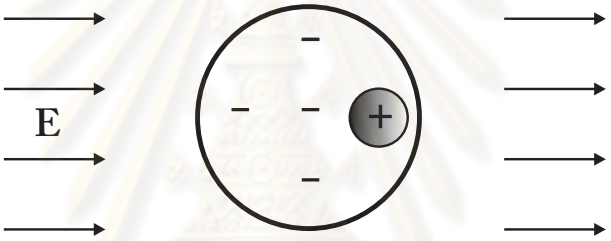

Figure 2.2: A polarized atom.

2.1.2 Linear Dielectrics

We consider the relation of the electric displacement (**D**), the electric field (**E**) and the polarization (**P**) as

$$\mathbf{D} = \varepsilon_0 \mathbf{E} + \mathbf{P}, \tag{2.1}$$

where ε_0 is called the permittivity of free space.

Generally, the dielectric property of linear and isotropic materials is that **P** is proportional to **E**. When **E** is not too strong, the relation between **P** and **E** can be written by

$$\mathbf{P} = \varepsilon_0 \chi' \mathbf{E}, \tag{2.2}$$

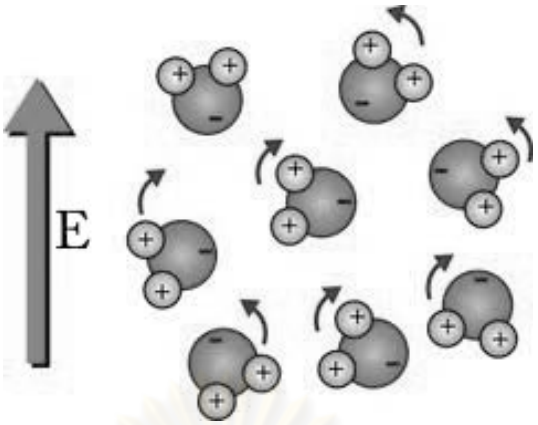

Figure 2.3: The polar molecules of water in an electric field.

where χ' is called the electric susceptibility which depends on the microscopic structure of the medium.

Substituting Eqs. (2.2) into (2.1), the alternative relation between $\mathbf{D}$ and $\mathbf{E}$ is given by

$$\begin{aligned} \mathbf{D} &= (1+\chi')\,\varepsilon_0\mathbf{E}, \\ &= \varepsilon\mathbf{E}, \end{aligned} \tag{2.3}$$

where $\varepsilon \equiv \varepsilon_0(1+\chi')$ is called the linear coefficient (or permittivity) of materials.

Therefore, the electric displacement is linearly proportional to the electric field in linear dielectric media.

2.1.3 Nonlinear Dielectrics

At large field intensities of about 10^6 V/m or higher, deviation of relation (2.3) becomes noticeable [33]. The nonlinear effects of the materials occur because of the interaction of the local field $\mathbf{E}$, with the molecular dipole moment, which rotates those dipoles and creates a polarization field $\mathbf{P}$. The polarization field is linearly dependent on the magnitude of the local field so long as they are small. This linearity eventually breaks down and higher order terms are needed to describe the polarization field. The polarization in this case is given by [34]

$$\mathbf{P} = \varepsilon_0\chi'\mathbf{E} + \varepsilon_0\chi'^{(3)}\left|\mathbf{E}\right|^2\mathbf{E} + \varepsilon_0\chi'^{(5)}\left|\mathbf{E}\right|^4\mathbf{E} + ..., \tag{2.4}$$

where χ', $\chi'^{(3)}$ and $\chi'^{(5)}$ are the nonlinear first, third and fifth order electric susceptibilities, respectively.

Thus, the nonlinear dielectrics are materials whose polarization is not proportional to the local electric field. Similarly, replacing Eqs. (2.4) into (2.1), the relation between the electric displacement ($\mathbf{D}$) and the electric field ($\mathbf{E}$) for nonlinear dielectric is

$$\mathbf{D} = \varepsilon\mathbf{E} + \chi |\mathbf{E}|^2 \mathbf{E} + ..., \tag{2.5}$$

where ε and χ are called the linear and nonlinear coefficients, respectively.

In this research, we concentrate on the nonlinear dielectric composites in which the relation between the electric displacement ($\mathbf{D}$) and the electric field ($\mathbf{E}$) obeys

$$\mathbf{D} = \varepsilon\mathbf{E} + \chi |\mathbf{E}|^\beta \mathbf{E}, \tag{2.6}$$

where β is nonlinear integer exponent.

Eq. (2.6) is assumed by $\varepsilon \gg \chi |\mathbf{E}|^\beta$ for weakly nonlinear composites and $\varepsilon \ll \chi |\mathbf{E}|^\beta$ for strongly nonlinear composites.

2.2 Basic Equations in Electrostatics

2.2.1 Laplace 's Equation

We consider the Maxwell's equations in electrostatics of dielectric media without free charge;

$$\nabla \cdot \mathbf{D} = 0 \tag{2.7}$$

and

$$\nabla \times \mathbf{E} = 0, \text{ or } \mathbf{E} = -\nabla\phi, \tag{2.8}$$

where ϕ is the electric potential.

By using Eqs. (2.3), (2.7) and (2.8), these lead to

$$\nabla^2\phi = 0. \tag{2.9}$$

This is Laplace's equation. The solution of Eq. (2.9) depends on the mathematical coordinates such as the elliptic cylindrical coordinates (u, v). The general solution is [35]

$$\phi(u,v) = \sum_{n=0}^{\infty} \left[(A_n \cosh(nu) + B_n e^{-nu}) \cos(nv) + (C_n \sinh(nu) + D_n e^{-nu}) \sin(nv) \right]. \tag{2.10}$$

where u and v are the variables in the elliptic cylindrical coordinates.

The solution of Laplace's equation in elliptic cylindrical coordinates is employed to determine the electric field inside the inclusion in Chapter 3.

2.2.2 Boundary Conditions

The boundary conditions are essential to be specified in solving for electric potentials in Chapter 3. These are as follows:

i) the electric potential in the host medium at remote distance,

ii) the electric field at the line between foci ($u = 0$) is parallel to the direction of the external uniform electric field,

iii) the continuity of the tangential component of the electric field at the inclusion surface,

iv) the continuity of the normal component of the electric displacement at the inclusion surface.

CHAPTER III

Composites with Identical Inclusion Shape

In this chapter, we investigate the effects of inclusion shapes on effective nonlinear responses of nonlinear elliptic cylindrical dielectric composites with identical inclusion shape in two dimensions. Three types of composites, linear, weakly nonlinear and strongly nonlinear, are considered. The effective linear coefficient (ε_e) of linear dielectric composites is determined. It is applied to determine the effective nonlinear coefficient (χ_e) of weakly and strongly nonlinear composites with the same microstructures as a linear composite by using the decoupling approximation. The effects of inclusion shapes on χ_e are reported for varying the aspect ratio (the ratios between the semi-major and semi-minor axes for identical inclusions).

3.1 Linear Dielectric Composites

3.1.1 Typical Structure and Model

We consider a linear composite which consists of linear elliptic cylindrical inclusions with identical shape, having the same aspect ratio, the ratio between major and minor axes ($M = c/b$), randomly oriented and embedded in a different linear dielectric medium in dilute limit, as shown in Figure 3.1. The linear coefficients of inclusions and medium are ε_i and ε_m, respectively. The axes of any inclusions are parallel and much longer than the respective semi major axes such that the system is considered as two dimensional.

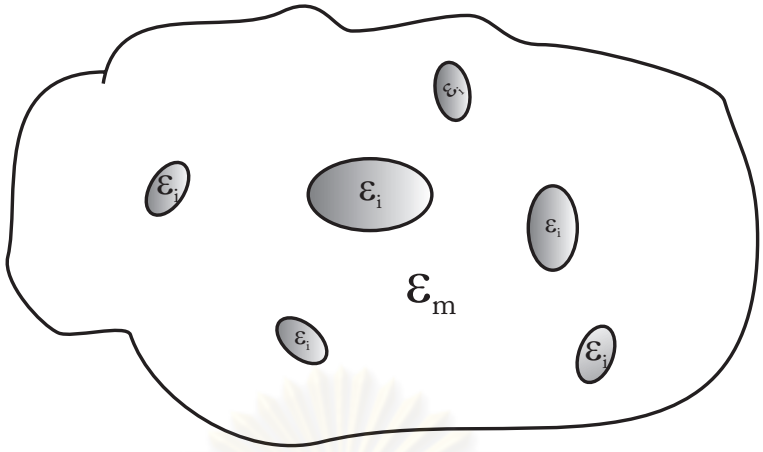

Figure 3.1: A linear dielectric composite with identical inclusion shape.

In the dilute limit or a low inclusion packing fraction (the ratio of inclusion volume to composite volume), the single inclusion model is assumed. Figure 3.2 shows the single inclusion model presented in elliptic cylindrical coordinates. The elliptic cylindrical inclusion is located at $0 \leq u \leq u_0$ and $0 \leq v \leq 2\pi$, where u and v are the variables in the elliptic cylindrical coordinate. $\widehat{u}$ and $\widehat{v}$ present the unit vectors in the normal component and tangential component of ellipse, respectively, as shown in Figure 3.3.

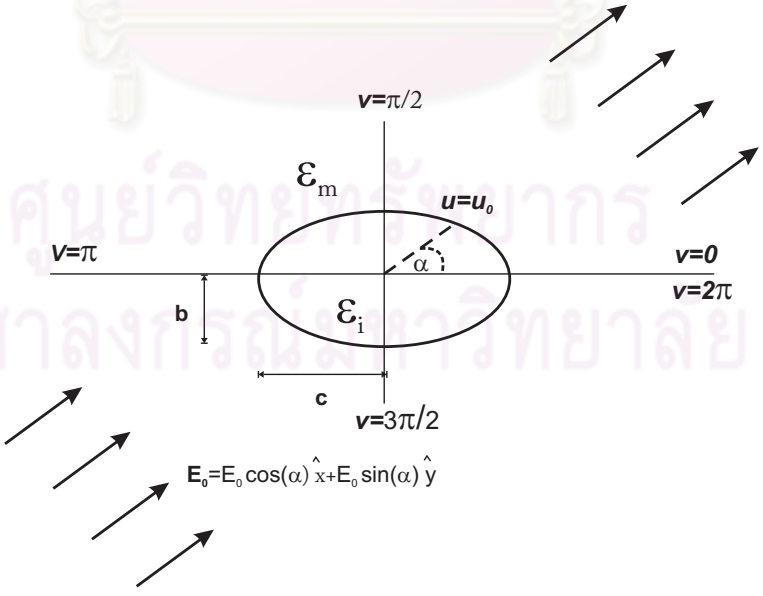

Figure 3.2: The single inclusion model of identical inclusion shape in elliptic cylindrical coordinates.

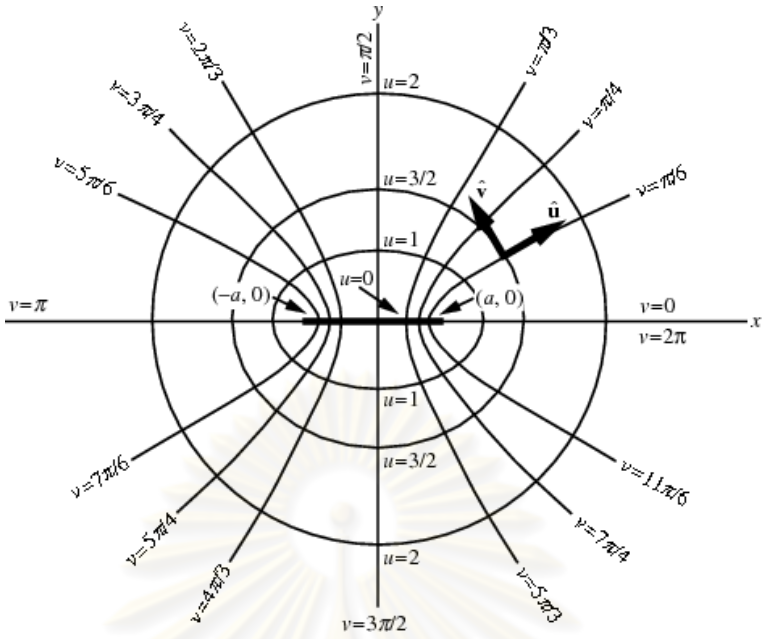

Figure 3.3: Elliptic Cylindrical Coordinates.

3.1.2 Electric Field inside Elliptic Cylindrical Inclusion

The electric field inside the elliptic cylindrical inclusion is required to determine the effective linear coefficient (ε_e). In the literature search, the electric field inside elliptic cylindrical inclusion was determined by Yu et al. [4] by using the complex transformation and conformal map. Alternatively, we present the determination of the electric field inside the elliptic cylindrical inclusion by using the elliptic cylindrical coordinates.

The electric potential inside an inclusion (ϕ) satisfies the Laplace equation:

$$\nabla^2\phi = 0. \tag{3.1}$$

We employ the elliptic cylindrical coordinates (u, v) which are related to the cartesian coordinates (x, y) by:

$$\begin{aligned} x &= a\cosh(u)\cos(v) \\ y &= a\sinh(u)\sin(v), \end{aligned}$$

where $a = \sqrt{c^2 - b^2}$ is the focal length of ellipse in Figure 3.2.

The general solution of Laplace's equation in elliptic cylindrical coordinates in this case is [35]

$$\phi(u,v) = \sum_{n=0}^{\infty} \left[(A_n \cosh(nu) + B_n e^{-nu}) \cos(nv) + (C_n \sinh(nu) + D_n e^{-nu}) \sin(nv) \right]. \tag{3.2}$$

In order to derive for the electric potentials in the inclusion and medium in Figure 3.2, the electric field is separated into two components $\widehat{x}$ and $\widehat{y}$ and the electric potentials are the linear superposition of the responses to both external fields, $E_{0x} = E_0 \cos(\alpha)$ and $E_{0y} = E_0 \sin(\alpha)$. The boundary conditions are given here as follows.

i) The electric potential in the host medium at remote distance ($u \to \infty$) becomes $-aE_{0x} \cosh(u) \cos(v)$. This omits the term of $n \neq 1$ and gives $A_1 = -aE_{0x}$.

ii) The electric potential is symmetric with respect to the x axis, $\phi(u,v) = \phi(u,-v)$. This omits the term of $\sin(v)$ because of $\sin(v) = -\sin(-v)$.

By using the two boundary conditions i) and ii), and the mathematical formula $\cosh(nu) - \sinh(nu) = e^{-nu}$, the electric potential in the host medium of the elliptic cylindrical inclusion with a major axis parallel to the external electric field is

$$\phi_m^x(u,v) = [-a \cosh(u) + B_1(\cosh(u) - \sinh(u))] \cos(v) E_{0x}. \tag{3.3}$$

Mathematically, at $u = 0$, it is a line connecting the two focal points of the cross section of the elliptic cylinder. Physically, when we apply the external electric field (E_{0x}) to the elliptic cylindrical inclusion located at $u = 0$, the electric field inside the inclusion occurs in the direction $\widehat{v}$ only. This is the boundary condition for determining the electric potential inside the inclusion.

As described above, if $u = 0$, the result of $\frac{\partial \phi_i(u,v)}{\partial u}|_{u=0} = 0$ gives the electric potential in the inclusion of the elliptic cylindrical inclusion with a major axis parallel to the external electric field:

$$\phi_i^x(u,v) = A_1^i \cosh(u) \cos(v) E_{0x}. \tag{3.4}$$

Similarly, when the external electric field $E_{0y} = E_0 \sin(\alpha)$ is applied perpendicular to the major axis of the inclusion, it can be proved that the electric potential in the host medium is

$$\phi_m^y(u,v) = [-a\sinh(u) + D_1(\cosh(u) - \sinh(u))]\sin(v)E_{0y}. \tag{3.5}$$

The electric potential inside the inclusion is

$$\phi_i^y(u,v) = C_1 \sinh(u)\sin(v)E_{0y}. \tag{3.6}$$

According to Figure 3.2, when the external electric field $\mathbf{E}_0 = E_0\cos(\alpha)\hat{x} + E_0\sin(\alpha)\hat{y}$, where α is the angle between $\mathbf{E}_0$ and the major axis of the inclusion aligned in the $\widehat{x}$ direction, is applied to the inclusion. From Eqs. (3.3) - (3.6), the electric potentials derived previously are modified to become

$$\phi_i^\alpha(u,v) = [A\cosh(u)\cos(v)\cos(\alpha) + B\sinh(u)\sin(v)\sin(\alpha)]\,E_0, \quad 0 \le u \le u_0 \tag{3.7}$$

$$\begin{aligned}\phi_m^\alpha(u,v) = {} & [-a\cosh(u) + C(\cosh(u) - \sinh(u))]\cos(v)\cos(\alpha)E_0 \\ & + [-a\sinh(u) + D(\cosh(u) - \sinh(u))]\sin(v)\sin(\alpha)E_0, \quad u_0 \le u < \infty.\end{aligned} \tag{3.8}$$

The constants A, B, C and D in Eqs. (3.7) and (3.8) can be determined by using the following boundary conditions at the inclusion surfaces:

iii) The tangential component of the electric field is continuous ($E_{1t} = E_{2t}$), then the electric potential is also continuous,

$$\phi_i^\alpha(u = u_0, v) = \phi_m^\alpha(u = u_0, v).$$

By using the relations $a\cosh(u_0) = c$ and $a\sinh(u_0) = b$, these lead to

$$A = -a + C\left(1 - \frac{b}{c}\right), \tag{3.9}$$

and

$$B = -a + D\left(\frac{c}{b} - 1\right). \tag{3.10}$$

iv) The normal component of the electric displacement is continuous ($D_{in} = D_{mn}$ or $\varepsilon_i E_{in} = \varepsilon_m E_{mn}$),

$$\varepsilon_i \frac{\partial \phi_i^\alpha}{\partial u}\,|_{u=u_0} = \varepsilon_m \frac{\partial \phi_m^\alpha}{\partial u}\,|_{u=u_0},$$

hence

$$\varepsilon_r A = -a + C(1 - \frac{c}{b}), \tag{3.11}$$

and

$$\varepsilon_r B = -a + D(\frac{b}{c} - 1), \tag{3.12}$$

where $\varepsilon_r = \varepsilon_i/\varepsilon_m$.

From Eqs. (3.9) - (3.12), the constants A, B, C, and D can be solved directly. The results are

$$A = \frac{-a\,(b+c)\,\varepsilon_m}{b\varepsilon_i + c\varepsilon_m}, \tag{3.13}$$

$$B = \frac{-a\,(b+c)\,\varepsilon_m}{b\varepsilon_m + c\varepsilon_i}, \tag{3.14}$$

$$C = \frac{c\,(b+c)}{a}\left[\frac{b(\varepsilon_i - \varepsilon_m)}{b\varepsilon_i + c\varepsilon_m}\right], \tag{3.15}$$

$$D = \frac{b\,(b+c)}{a}\left[\frac{c(\varepsilon_i - \varepsilon_m)}{b\varepsilon_n + c\varepsilon_i}\right]. \tag{3.16}$$

Next, the gradient in elliptic cylindrical coordinate is used to calculate the electric field inside the inclusion $\mathbf{E}_i^\alpha = -\nabla\phi_i^\alpha(u,v)$. The gradient is

$$\nabla = \frac{1}{ah}\left[\hat{u}\frac{\partial}{\partial u} + \hat{v}\frac{\partial}{\partial v}\right], \tag{3.17}$$

where $h = \sqrt{\frac{\cosh(2u)-\cos(2v)}{2}}$.

We obtain

$$\begin{aligned}\mathbf{E}_i^\alpha(u,v) = &-\frac{E_0}{ah}\left[A\sinh(u)\cos(v)\cos(\alpha) + B\cosh(u)\sin(v)\sin(\alpha)\right]\hat{u} \\ &-\frac{E_0}{ah}\left[-A\cosh(u)\sin(v)\cos(\alpha) + B\sinh(u)\cos(v)\sin(\alpha)\right]\hat{v}.\end{aligned} \tag{3.18}$$

This is unfamiliar and inappropriate form for determining the effective linear coefficient ε_e, because the external electric field is applied in the cartesian coordinates and the major axis of inclusion aligns in x axis. To obtain $\mathbf{E}_i^\alpha(u,v)$ in the cartesian coordinates, the relationships between unit vectors $\hat{u}$ and $\hat{v}$ in elliptic cylindrical coordinates and those of $\hat{x}$ and $\hat{y}$ in cartesian coordinates are used. These are

$$\hat{u} = \frac{1}{h}\left[\sinh(u)\cos(v)\hat{x} + \cosh(u)\sin(v)\hat{y}\right], \tag{3.19}$$

$$\hat{v} = \frac{1}{h}\left[-\cosh(u)\sin(v)\hat{x} + \sinh(u)\cos(v)\hat{y}\right]. \tag{3.20}$$

By replacing Eqs.(3.19) and (3.20) into (3.18), we have

$$\mathbf{E}_i^{\alpha}(x,y) = \frac{-E_0}{a}\left[A\cos\alpha\hat{x} + B\sin\alpha\hat{y}\right]. \tag{3.21}$$

Substituting the constants A and B of Eqs. (3.13) and (3.14) into Eq. (3.21), we get

$$\mathbf{E}_i^{\alpha} = E_0(b+c)\varepsilon_m\left[\frac{\cos\alpha\widehat{x}}{b\varepsilon_i + c\varepsilon_m} + \frac{\sin\alpha\widehat{y}}{c\varepsilon_i + b\varepsilon_m}\right]. \tag{3.22}$$

We note that Eq. (3.22) confirms the electric field inside the elliptic cylindrical inclusion ($\mathbf{E}_i^{\alpha}$) reported by Yu et al. [4].

3.1.3 Effective Linear Coefficient

The average field method proposed by Landau and Lifshitz [40] is used to determine the effective linear dielectric coefficient (ε_e) which yields:

$$\frac{1}{V}\int_V \left[\mathbf{D} - \varepsilon_m\mathbf{E}\right] dV = \overline{\mathbf{D}} - \varepsilon_m\overline{\mathbf{E}}, \tag{3.23}$$

where $\overline{\mathbf{E}}$ is the volume average of electric field in the composite constituents, $\overline{\mathbf{E}} = (1/V)\int_V \mathbf{E}dV$, and V is the composite volume. The effective linear coefficient is defined as $\overline{\mathbf{D}} = \varepsilon_e\overline{\mathbf{E}}$, where $\overline{\mathbf{D}}$ is the volume average of electric displacement. From the boundary condition of electric potential on the composite surface at $-\mathbf{E}_0\cdot\mathbf{x}$ where $\mathbf{x}$ is the position vector on the composite surface, it can be shown that $\overline{\mathbf{E}} = \mathbf{E}_0$. Thus equation (3.23) becomes

$$\frac{1}{V}\int_{V_i}(\varepsilon_i - \varepsilon_m)\mathbf{E}_i dV = (\varepsilon_e - \varepsilon_m)\mathbf{E}_0, \tag{3.24}$$

where V_i is the inclusion domain. The effective linear coefficient (ε_e) is therefore given by

$$\varepsilon_e = \varepsilon_m + \frac{(\varepsilon_i - \varepsilon_m)}{VE_0^2}\mathbf{E}_0\cdot\int_{V_i}\mathbf{E}_i dV. \tag{3.25}$$

Substituting $\mathbf{E}_0 = E_0\cos(\alpha)\widehat{x} + E_0\sin(\alpha)\widehat{y}$ and $\mathbf{E}_i$ from Eqs. (3.22) into (3.25) yields

$$\varepsilon_e^{\alpha} = \varepsilon_m\left[1 + v_i(\varepsilon_i - \varepsilon_m)(b+c)\left(\frac{\cos^2(\alpha)}{b\varepsilon_i + c\varepsilon_m} + \frac{\sin^2(\alpha)}{c\varepsilon_i + b\varepsilon_m}\right)\right], \tag{3.26}$$

where $v_i = V_i/V$ is the inclusion packing fraction.

Note that from Eq. (3.26), for an applied electric field parallel ($\alpha = 0^0$) or perpendicular ($\alpha = 90^0$) to the major axis of inclusion, it leads to Eqs. (21) and (22), respectively, as reported by Wei et al. [35]. They have investigated the effective dielectric responses of elliptical graded cylindrical composites in the dilute limit under the external electric field. Because the electric fields are applied along $\widehat{x}$ and $\widehat{y}$ directions separately, any elliptic cylindrical inclusions are not randomly oriented.

For totally randomly oriented elliptical inclusions, the angular average of ε_e^{α} in Eq. (3.26) is performed to give

$$\varepsilon_e/\varepsilon_m = \left[1 + \frac{v_i}{2}(\varepsilon_r - 1)(1 + M)\left(\frac{1}{\varepsilon_r + M} + \frac{1}{M\varepsilon_r + 1}\right)\right], \qquad (3.27)$$

where v_i is the volume packing fraction of inclusions, $\varepsilon_r = \varepsilon_i/\varepsilon_m$ and $M = c/b$.

Moreover, for $b = c$ ($M = 1$), Eq. (3.27) is also reduced to the well-known result of a linear cylindrical dielectric composite in the dilute limit of $\varepsilon_e = \varepsilon_m\left[1 + 2v_i\frac{(\varepsilon_i - \varepsilon_m)}{(\varepsilon_i + \varepsilon_m)}\right]$. The effective linear coefficient (ε_e) of Eq. (3.27) is required to determine the effective nonlinear coefficients (χ_e) of strongly nonlinear elliptical composites by using the decoupling approximation in the next section.

3.1.4 Results and Discussion

In Figure 3.4, the relative effective linear coefficients ($\varepsilon_e/\varepsilon_m$) from Eq. (3.27) are shown on the logarithmic scale for varying the linear contrast (ε_r) with the aspect ratio (M) as parameter for the inclusion packing fraction (v_i) of 0.08. The results show the increase in $\varepsilon_e/\varepsilon_m$ with increasing the aspect ratio (M) within the range of $log(\varepsilon_r) > 0.3$ (or $\varepsilon_r \gg 2.0$). In contrast, within the range of $log(\varepsilon_r) < -0.3$ (or $\varepsilon_r \ll 0.5$), increasing the aspect ratio reduces the effective linear coefficient ε_e. For small linear contrast (ε_r), $-0.3 \leq log(\varepsilon_r) \leq 0.3$ (or $0.5 \leq \varepsilon_r \leq 2.0$), increasing the aspect ratio does not affect ε_e of linear elliptical composites.

Figure 3.5 shows the relative effective linear coefficients ($\varepsilon_e/\varepsilon_m$) for varying the aspect ratio (M) with the linear contrast (ε_r) as parameter. The result reveals

the increase in $\varepsilon_e/\varepsilon_m$ with increasing ε_r. For $\varepsilon_r = 10$, increasing M slightly affect $\varepsilon_e/\varepsilon_m$ within the range of $1 \leq M \leq 100$. In contrast, for $\varepsilon_r = 100$ and 1000, increasing M tremendously affect $\varepsilon_e/\varepsilon_m$. For higher ε_r, $\varepsilon_e/\varepsilon_m$ rapidly increases to the value which depends on varying parameter M. As seen from Eq. (3.27), ε_e becomes more dependent on M as high ε_r.

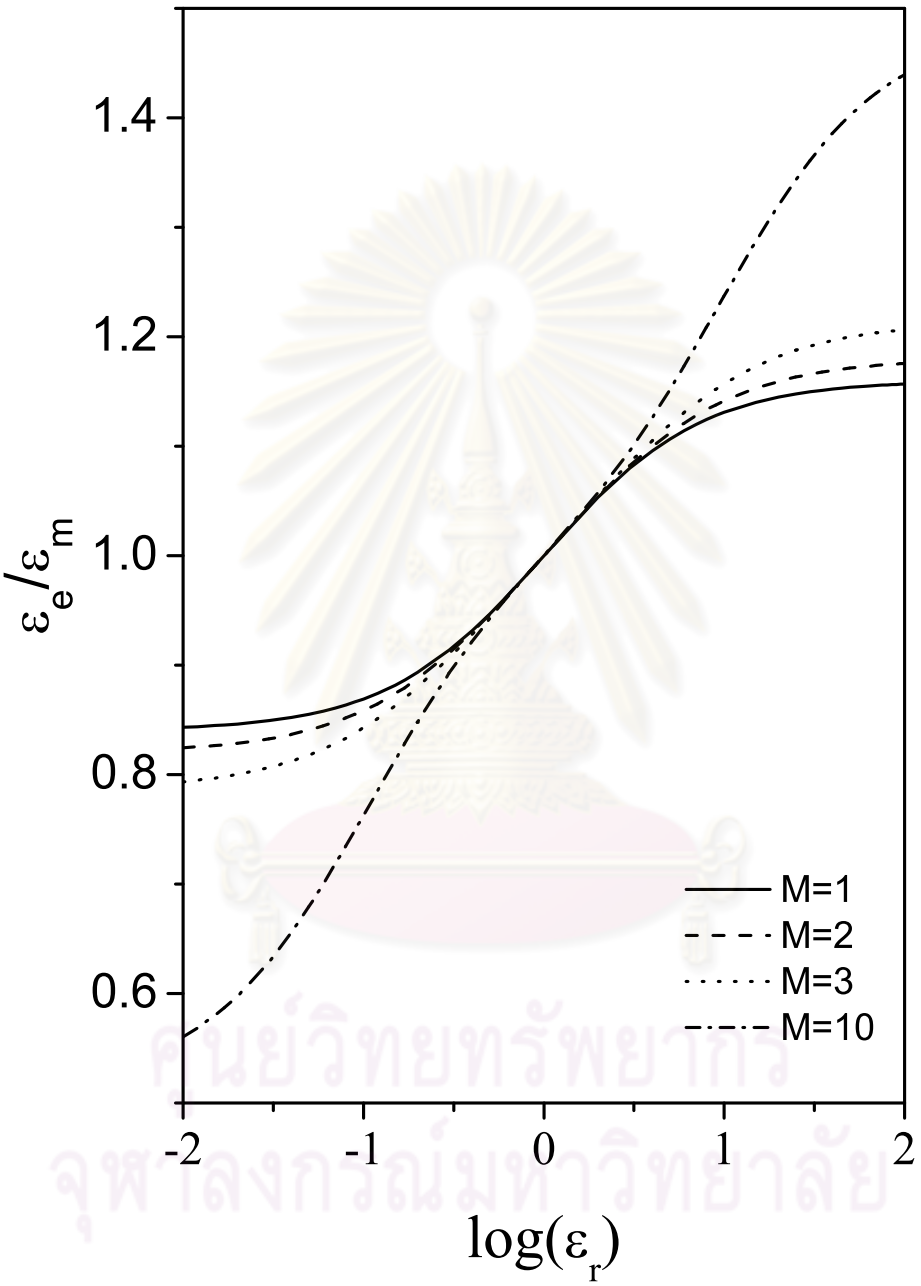

Figure 3.4: The relative effective linear coefficients ($\varepsilon_e/\varepsilon_m$) for varying the linear contrast (ε_r) with the aspect ratio (M) as parameter and an inclusion packing fraction (v_i) = 0.08.

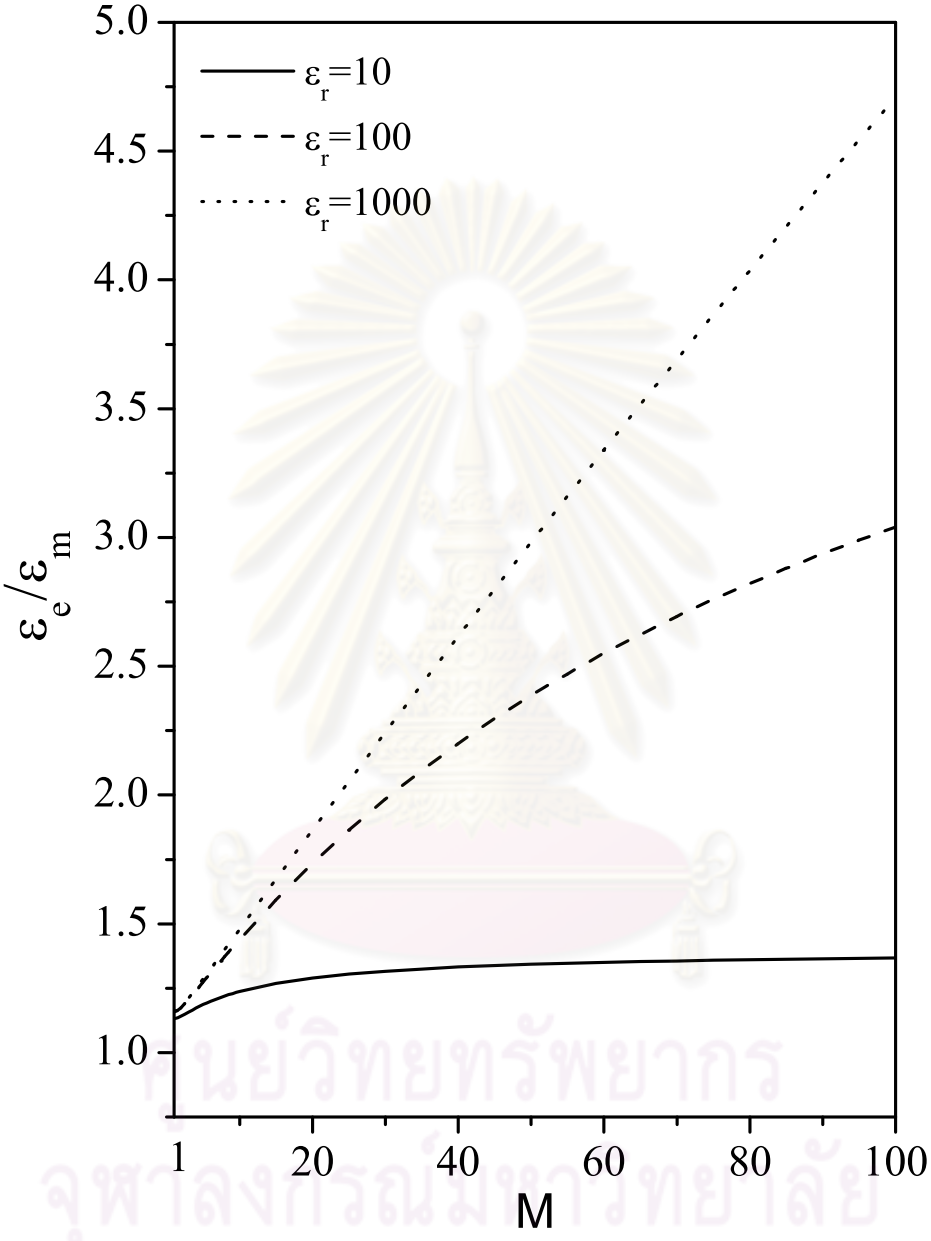

Figure 3.5: The relative effective linear coefficients ($\varepsilon_e/\varepsilon_m$) for varying the aspect ratio (M) with the linear contrast (ε_r) as parameter and an inclusion packing fraction (v_i) = 0.08.

3.2 Weakly Nonlinear Dielectric Composites

3.2.1 Typical Structure

We consider a nonlinear composite with identical inclusion shape in two dimensions, which has the same microstructure as in linear dielectric composite described in the previous section. The composite consists of weakly nonlinear elliptic cylindrical inclusions with identical shape, having the same aspect ratio (the ratio between semi-major and semi-minor axes, $M = c/b$), randomly oriented and embedded in a linear dielectric medium in dilute limit. The relation between the electric displacement ($\mathbf{D}$) and electric field ($\mathbf{E}$) inside the inclusions has the form $\mathbf{D} = \varepsilon\mathbf{E} + \chi|\mathbf{E}|^\beta\mathbf{E}$ where β is a nonlinear integer exponent and $\chi|\mathbf{E}|^\beta \ll \varepsilon$. The linear and nonlinear coefficients of inclusions and medium are ε_i, χ_i and ε_m, $\chi_m = 0$, respectively. Figure 3.6 shows a weakly nonlinear dielectric composite with identical inclusion shape.

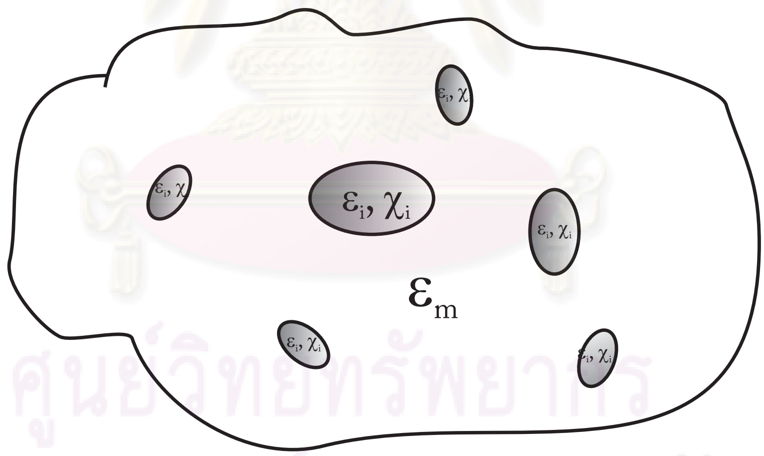

Figure 3.6: A weakly nonlinear dielectric composite with identical inclusion shape.

3.2.2 Effective Nonlinear Coefficient

For weakly nonlinear dielectric composite, the nonlinear response is small compared to the linear response. We consider the work of Hui and Chung [11]

which has the same basic relation between the electric displacement ($\mathbf{D}$) and electric field ($\mathbf{E}$) as this thesis. They have studied the effective nonlinear response in random composites consisting of weakly nonlinear cylindrical (and spherical) inclusions randomly embedded in the host medium with arbitrary nonlinear integer exponents. By using the effective medium approximation, the expression of effective nonlinear coefficient (χ_e) with arbitrary nonlinear integer exponents was derived. In this section, we follow their method in deriving the effective nonlinear coefficient (χ_e).

The effective nonlinear coefficient (χ_e) can be defined by using the average energy method [11]. The energy of effective medium is defined by $W = \int \mathbf{D}\cdot\mathbf{E}dV$, which equals the sum of the energy of the inclusion and medium.

$$\begin{aligned}\chi_e E_0^{\beta+2} V &= \int_{V_i} \chi_i(x)\left|\mathbf{E}_i(x)\right|^{\beta+2} dV + \int_{V_m} \chi_m(x)\left|\mathbf{E}_m(x)\right|^{\beta+2} dV, \\ &= \frac{v_i\chi_i\left\langle E_i^{\beta+2}\right\rangle_i}{E_0^{\beta+2}} + \frac{v_m\chi_m\left\langle E_m^{\beta+2}\right\rangle_m}{E_0^{\beta+2}}, \end{aligned} \tag{3.28}$$

where $v_i = V_i/V$ and $\left\langle E_i^{\beta+2}\right\rangle = (1/V_i)\int_{V_i}|\mathbf{E}_i|^{\beta+2}dV$.

The subscripts i and m outside the brackets denote the average over the inclusion and medium regions, respectively. For convenience, we omit them because the subscripts also appear in the electric field.

For our case of linear medium ($\chi_m = 0$), the effective nonlinear coefficient (χ_e) is

$$\chi_e = \frac{1}{E_0^{\beta+2}}\left(v_i\chi_i\langle E_i^{\beta+2}\rangle\right), \tag{3.29}$$

where E_i is the linear electric field inside inclusion and v_i is the inclusion volume packing fractions.

In fact, the problem in calculation the values of χ_e is that of the determination of the volume average of electric field to the power $\beta+2$, $\langle E_i^{\beta+2}\rangle$ in the inclusion. There are several methods to obtain $\langle E_i^{\beta+2}\rangle$ depending on the nature of problem and the types of composites. If we determine $\langle E_i^{\beta+2}\rangle$ based on the average energy method and the average field method, we must obtain the analytical form of the electric field solutions which are more complex and difficult.

In this research, we are interested in the methods which simplify the calculation. The simple decoupling approximation, the improved decoupling approximation and the direct method have been employed.

A. Simple Decoupling Approximation

The (simple) decoupling approximation was originally proposed by Stroud and Wood [13] and has been widely applied to study nonlinear composites by many authors [9, 14, 21, 28]. This method directly relates the result of linear response to the nonlinear one for the composite with the same microstructure. Moreover, it also give an approximates $\langle E_i^{\beta+2} \rangle$ in Eq. (3.29) as

$$\langle E_i^{\beta+2} \rangle \approx \langle E_i^2 \rangle^{(\beta+2)/2}. \tag{3.30}$$

The effective nonlinear coefficient (χ_e) in Eq. (3.30) is alternatively derived in terms of the volume average of electric field to the second power $\langle E_i^2 \rangle$, which simplifies the calculation. $\langle E_i^2 \rangle$ is evaluated by using the derivative of effective linear coefficients (ε_e) with respect to linear coefficient of inclusion,

$$\left\langle E_i^2 \right\rangle = \frac{1}{v_i} \frac{\partial \varepsilon_e}{\partial \varepsilon_i} E_0^2. \tag{3.31}$$

By using Eq. (3.27) - (3.31), the effective nonlinear coefficients (χ_e) are obtained in terms of χ_i, ε_r, v_i, β and M.

B. Improved Decoupling Approximation

However, the estimate χ_e from $\langle E_i^{\beta+2} \rangle \approx \langle E_i^2 \rangle^{(\beta+2)/2}$ by using the simple decoupling approximation, is less than the exact value. These is confirmed by our theoretical prediction that $\chi_e(exact) \geq \chi_e(decoupling)$ reported in reference [14, 44]. We previously determined the effective nonlinear coefficient χ_e of strongly nonlinear spherical dielectric composites by using the simple decoupling approximation [14]. In order to analyze the validity, our results of χ_e are compared with the experimental results by Gehr et al. [15]. They reported the relative effective nonlinear coefficient (χ_e/χ_{fluid}) of porous-glass-based composites with silica glass

70 % and spaces 28%. The spaces in the sample were replaced by various nonlinear fluid, such as methanol, carbon tetrachloride and diiodomethane. The relative nonlinear coefficients of glass ($\chi_{glass}/\chi_{fluid}$) are 0.62, 0.32, and 0.03, respectively. In comparison, our results which predict the effective nonlinear coefficient are lower than the experimental results, which also confirm the theoretical prediction $\chi_e(exact) \geq \chi_e(decoupling)$.

In this section, we aim to use the improved decoupling approximation proposed by Lu and Li [12] for determining χ_e. Their work is the extension of the work of Hui and Chung [11], which proposed the method to improve mathematical derivation of $\langle E_i^{\beta+2} \rangle$. In the improved decoupling approximation, when n is odd and $n \geq 3$,

$$\langle (E_i - \langle E_i \rangle)^n \rangle = 0. \tag{3.32}$$

For n is even;

$$\langle (E_i - \langle E_i \rangle)^n \rangle \approx \left\langle (E_i - \langle E_i \rangle)^2 \right\rangle^{n/2}. \tag{3.33}$$

These was applied to derive the effective nonlinear coefficient of cylindrical composites with $\beta = 3, 4, 5$ and 6 given in reference [12] by using the effective medium approximation. In this research, from Eqs. (3.32) and (3.33), the more accurate expressions of $\left\langle E_i^{\beta+2} \right\rangle$ are given in terms of $\langle E_i^2 \rangle$ and $\langle E_i \rangle$ which the derivation is shown Appendix A. We obtain

$$\left\langle E_i^3 \right\rangle = 3 \left\langle E_i^2 \right\rangle \langle E_i \rangle - 2 \langle E_i \rangle^3, \tag{3.34}$$

$$\left\langle E_i^4 \right\rangle \approx 4 \left\langle E_i^2 \right\rangle \langle E_i \rangle^2 - 4 \langle E_i \rangle^4 + \left\langle E_i^2 \right\rangle^2, \tag{3.35}$$

$$\left\langle E_i^5 \right\rangle \approx 5 \left\langle E_i^2 \right\rangle^2 \langle E_i \rangle - 4 \langle E_i \rangle^5, \tag{3.36}$$

$$\left\langle E_i^6 \right\rangle \approx 12 \left\langle E_i^2 \right\rangle^2 \langle E_i \rangle^2 - 12 \left\langle E_i^2 \right\rangle \langle E_i \rangle^4 + \left\langle E_i^2 \right\rangle^3, \tag{3.37}$$

$$\left\langle E_i^7 \right\rangle \approx 14 \left\langle E_i^2 \right\rangle^2 \langle E_i \rangle^3 - 28 \left\langle E_i^2 \right\rangle \langle E_i \rangle^5 + 7 \left\langle E_i^2 \right\rangle^3 \langle E_i \rangle + 8 \langle E_i \rangle^7, \tag{3.38}$$

and

$$\left\langle E_i^8 \right\rangle \approx 24 \left\langle E_i^2 \right\rangle^3 \langle E_i \rangle^2 - 8 \left\langle E_i^2 \right\rangle^2 \langle E_i \rangle^4 - 32 \left\langle E_i^2 \right\rangle \langle E_i \rangle^6 + 16 \langle E_i \rangle^8 + \left\langle E_i^2 \right\rangle^4. \tag{3.39}$$

Now, $\left\langle E_i^\beta \right\rangle$ is presented in terms of $\langle E_i^2 \rangle$ and $\langle E_i \rangle$, which simplifies the calculations of χ_e. Eqs. (3.34) - (3.39) are substituted into Eq. (3.29) in order to determine

the more accurate effective nonlinear coefficient (χ_e) with the nonlinear integer exponents $\beta = 2, 4$ and 6.

$\langle E_i \rangle$ is evaluated from Eq. (3.22) with the definition $\langle E_i \rangle = (1/V_i) \int_{V_i} |\mathbf{E}_i| dV$, where V_i is the inclusion volume. In addition, $\langle E_i^2 \rangle$ is evaluated by using the simple decoupling approximation with Eqs. (3.26) and (3.31).

After the calculation described above, the effective nonlinear coefficients (χ_e^α) are obtained in terms of χ_i, ε_r, v_i, β, M and α. For totally randomly oriented elliptical inclusions, the angular average of effective nonlinear coefficient (χ_e^α) is used

$$\chi_e = \frac{1}{2\pi} \int_0^{2\pi} \chi_e^\alpha d\alpha. \tag{3.40}$$

We then obtain the effective nonlinear coefficient (χ_e) in terms of χ_i, ε_r, v_i, β and M, as needed.

C. Direct Method

In order to compare the values of χ_e calculated by using both methods, A and B, and to check the reliability, we also calculate χ_e directly by using the direct method based on reference [4]. This method use the average energy method to define χ_e in terms of the close form of electric potential. Therefore, it provides the accurate result of χ_e. However, the direct calculation of χ_e has difficulty in determination of $\left\langle E_i^{\beta+2} \right\rangle$ because of the complicated mathematical process.

In calculation, we also use the information of a linear composite as in section 3.1, which has the same microstructure as considered in weakly nonlinear elliptical dielectric composite. To determine the volume average of electric field $\left\langle E_i^{\beta+2} \right\rangle$, the direct integration is

$$\left\langle E_i^{\beta+2} \right\rangle = (1/V_i) \int_{V_i} |\mathbf{E}_i^{\beta+2}| dV, \tag{3.41}$$

where $\mathbf{E}_i = E_0(b+c)\varepsilon_m \left[\frac{\cos(\alpha)\widehat{x}}{b\varepsilon_i + c\varepsilon_m} + \frac{\sin(\alpha)\widehat{y}}{c\varepsilon_i + b\varepsilon_m} \right]$.

Substituting the result of integration in Eq. (3.41) into Eq. (3.29), we obtain the effective nonlinear coefficients (χ_e^α) in terms of α. Then, the angular average

results χ_e are used to predict the effective response of composite in terms of χ_i, ε_r, v_i, β and M, as parameters.

3.2.3 Results and Discussion

By using the decoupling approximation, we obtain the relative effective nonlinear coefficients (χ_e/χ_i) for the composites consisting of weakly nonlinear elliptic cylindrical inclusions with nonlinear integer exponents $\beta = 2$, 4 and 6, and inclusion packing fraction (v_i) of 0.08, as shown in Figure 3.7. For the linear contrast (ε_r) less than 1, i.e. $\varepsilon_r = 0.1$, the results show the increase in χ_e/χ_i with increasing β, in contrast, for ε_r larger than 1, i.c. $\varepsilon_r = 10$, increasing β resulting in decreasing χ_e/χ_i. The increase (and decrease) in χ_e/χ_i for varying the contrast (ε_r) is due to the electric field inside the dielectric inclusion is stronger (and weaker) than the applied electric field for ε_r is less (and larger) than 1. For both ranges of ε_r smaller and larger than 1, the effect of varying the aspect ratio (M) upon the relative effective nonlinear coefficients (χ_e/χ_i), reveals the rapid increase in χ_e/χ_i with increasing the aspect ratio within the range of $M \leq 50$. In contrast, within the range of $M > 50$, increasing the aspect ratio affects the slow increasing χ_e of the composites.

In Figure 3.8, the effect of varying the linear contrast ε_r, upon χ_e/χ_i is shown, within the range of $0 \leq \varepsilon_r \leq 1$, an inclusion packing fraction (v_i) of 0.08, for nonlinear integer exponent (β) = 2, 4 and 6, and the aspect ratio from 1 to 10 as parameter. The results show the significant decrease in χ_e/χ_i with increasing ε_r. For ε_r approaches 1, χ_e/χ_i slowly decreases to the same value independent of varying parameter M from 1 to 10. As seen from Eq. (3.27), ε_e becomes less dependent on M as ε_r approaches 1.

We note that for $\beta = 2$, our results of χ_e/χ_i concur with Eq. (22) of Yu, Hui and Stroud [4] predicting the effective third order coefficient (χ_e) of weakly nonlinear elliptical dielectric composite and confirm their result that $\chi_e/\chi_i = v_i$ at $\varepsilon_r = 1$. For $\beta = 4$, the result of χ_e/χ_i is a special case of that proposed by Potisook and Natenapit (to be published elsewhere) in the studying of higher-

order weakly nonlinear response of elliptic cylindrical composites. Moreover, we also determine the relative effective nonlinear coefficients (χ_e/χ_i) for $\beta = 2, 4$ and 6 by using the improved decoupling approximation which determined χ_e with the more accurate mathematical formulae than the simple decoupling approximation based on reference [12] in part B and the direct method which determines χ_e directly without the decoupling approximation based on reference [4] in part C. These give the same results of χ_e, as expected, since the electric field in inclusions is uniform. Therefore, the decoupling approximation is actually exact.

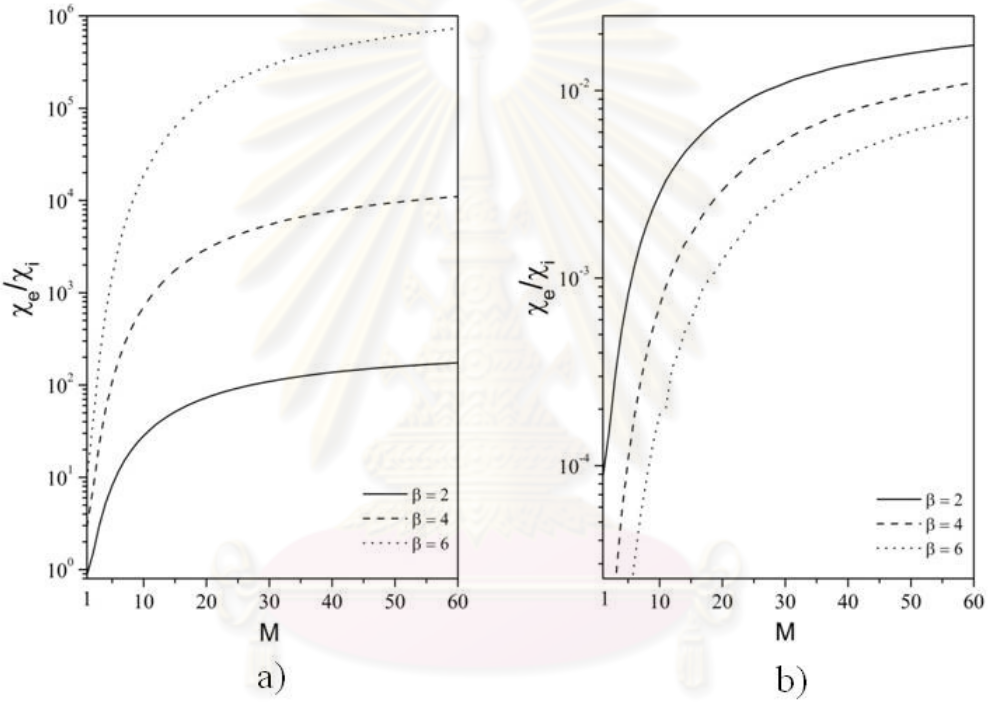

Figure 3.7: The relative effective nonlinear coefficients (χ_e/χ_i) for varying the aspect ratio with the nonlinear integer exponent (β) as parameter for the contrast (ε_r) equal to a) $\varepsilon_r = 0.1$ and b) $\varepsilon_r = 10$.

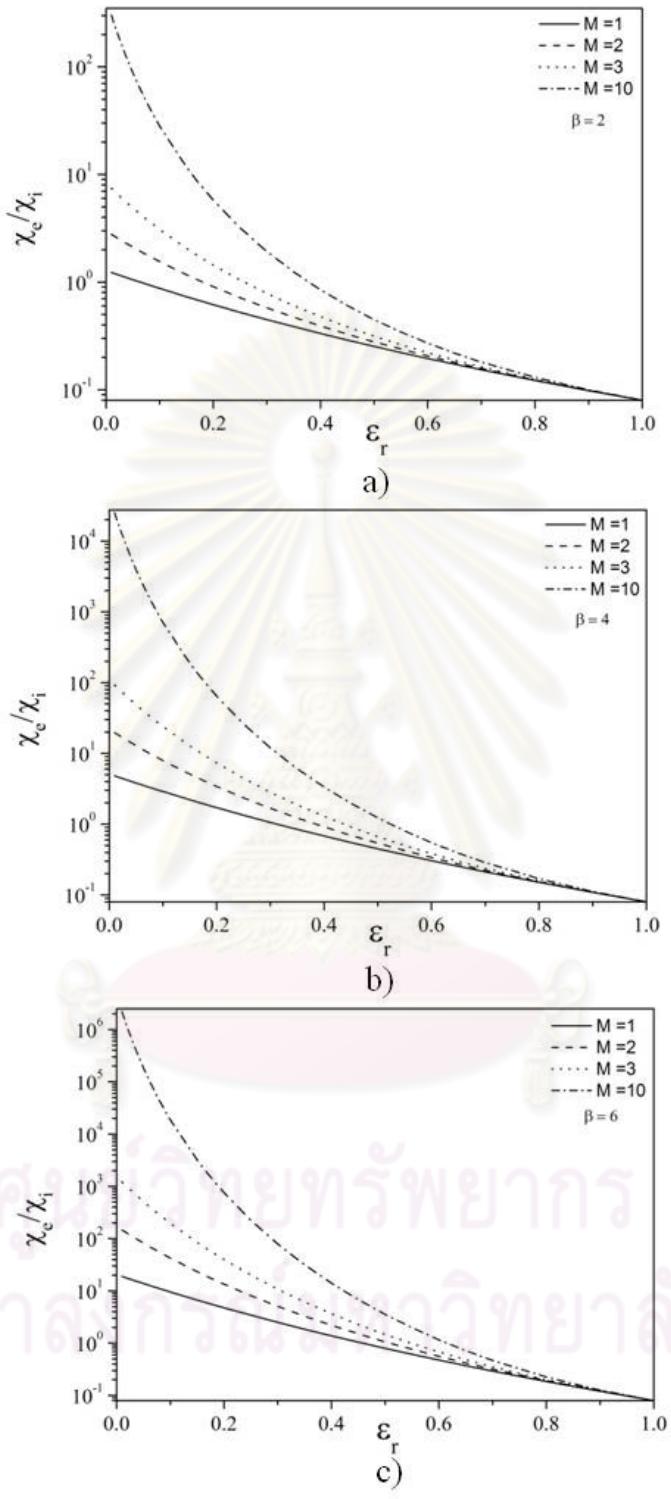

Figure 3.8: The relative effective nonlinear coefficients (χ_e/χ_i) for varying the contrast (ε_r) with the aspect ratio (M) as parameter for the nonlinear integer exponent (β) equal to a) $\beta = 2$, b) $\beta = 4$ and c) $\beta = 6$.

3.3 Strongly Nonlinear Dielectric Composites

3.3.1 Typical Structure

In this section, we theoretically investigate the effect of variation of the inclusion shapes on the effective nonlinear coefficients of strongly nonlinear elliptical dielectric composites. It is assumed that the relationship between the electric displacement and the electric field for both inclusions and medium obey the form $\mathbf{D} = \varepsilon\mathbf{E} + \chi|\mathbf{E}|^2\mathbf{E}$ where $\varepsilon \ll \chi|\mathbf{E}|^2$ is of interest. The composite consists of parallel elliptical strongly nonlinear dielectric inclusions having the same aspect ratio (the ratio between semi major and semi minor axes, $M = c/b$) with the cross-sections randomly oriented and embedded in a different strongly nonlinear dielectric medium in the dilute limit, as shown in Figure 3.9. The axes of any inclusions are much longer than the respective semi major axis such that the system is, therefore, considered as two dimensional.

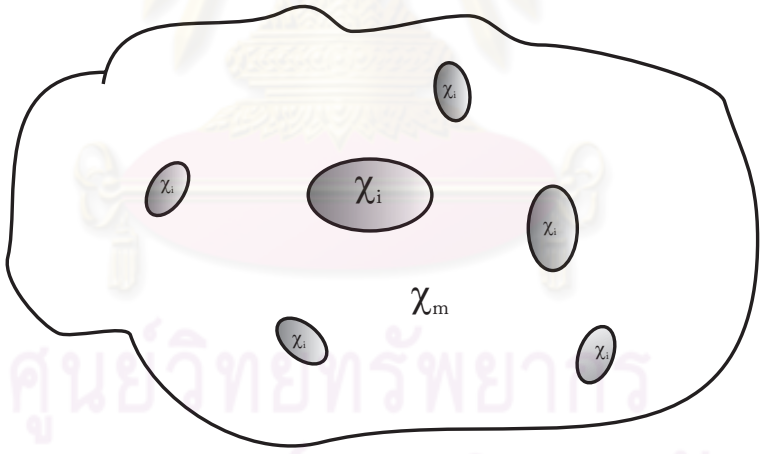

Figure 3.9: A strongly nonlinear dielectric composite with identical inclusion shape.

3.3.2 Effective Nonlinear Coefficient

The decoupling approximation has been previously applied to investigate the effective response of strongly nonlinear cylindrical and spherical composites with

dilute packing fractions by Gao and Li [38]. In their work, the effective nonlinear coefficient (χ_e) of composites has been predicted with the relation between the electric displacement ($\mathbf{D}$) and electric field ($\mathbf{E}$) of the form $\mathbf{D} = \chi|\mathbf{E}|^2\mathbf{E}$. Following their work, we further determine the effective nonlinear coefficient (χ_e) of strongly nonlinear elliptic cylindrical dielectric composites and to investigate the shape effects of inclusions upon the value of χ_e.

By using the average energy method, the energy of effective medium equals the sum of the energy of the inclusion and medium. The effective nonlinear coefficient (χ_e) of composites is [9]

$$\begin{aligned} \chi_e &= \frac{1}{E_0^4 V}\left[\int_{V_i} \chi_i(x)\left|\mathbf{E}_i(x)\right|^4 dV + \int_{V_m} \chi_m(x)\left|\mathbf{E}_m(x)\right|^4 dV\right] \\ &= \frac{v_i\chi_i\left\langle E_i^4\right\rangle}{E_0^4} + \frac{v_m\chi_m\left\langle E_m^4\right\rangle}{E_0^4}. \end{aligned} \tag{3.42}$$

where E_i and E_m are the linear electric fields inside the inclusion and medium, respectively, subject to the same boundary conditions and same microstructure as considered in linear composites in section 2.1. v_i and $v_m = 1 - v_i$ are the inclusion and medium volume fractions, respectively.

We invoke the simple decoupling approximation as given by Eq. (3.30) for $\beta = 2$, assuming that $\langle E_i^4\rangle \approx \langle E_i^2\rangle^2$ and $\langle E_m^4\rangle \approx \langle E_m^2\rangle^2$ [9]. The effective nonlinear coefficients (χ_e) of composites can be determined from the relationship

$$\chi_e = \frac{v_i\chi_i\left\langle E_i^2\right\rangle^2}{E_0^4} + \frac{v_m\chi_m\left\langle E_m^2\right\rangle^2}{E_0^4}. \tag{3.43}$$

The relations between the volume average of electric fields to the second power in the inclusions and host medium and the derivative of the effective linear coefficients are given as [9]:

$$\left\langle E_i^2\right\rangle = \frac{1}{v_i}\frac{\partial\varepsilon_e}{\partial\varepsilon_i}E_0^2, \tag{3.44}$$

$$\left\langle E_m^2\right\rangle = \frac{1}{v_m}\frac{\partial\varepsilon_e}{\partial\varepsilon_m}E_0^2, \tag{3.45}$$

where $\mathbf{E}_0$ is the external uniform electric field.

Substituting ε_e^α as given by Eq. (3.26) into Eqs. (3.44) and (3.45), we obtain the equations for determining $\langle E_i^2\rangle$ and $\langle E_m^2\rangle$ in terms of the aspect ratios

($M = c/b$), inclusion packing fraction (v_i), the nonlinear contrast ($\chi_r = \chi_i/\chi_m$) and the angle α. By using the relations $\varepsilon_e = \chi_e E_0^2$, $\varepsilon_i = \chi_i \langle E_i^2 \rangle$ and $\varepsilon_m = \chi_m \langle E_m^2 \rangle$ [9], then $\langle E_i^2 \rangle$ and $\langle E_m^2 \rangle$ can be solved self-consistently depending on α. Replacing the latter $\langle E_i^2 \rangle$ and $\langle E_m^2 \rangle$, we obtain χ_e in terms of α. Then, the angular average results of χ_e are used to predict the effective response of composite in terms of χ_r, v_i, β and M, as parameters.

3.3.3 Results and Discussion

By using the decoupling approximation, we obtain the relative effective nonlinear coefficients (χ_e/χ_m) for composites with elliptic cylindrical inclusion with packing fractions (v_i) of 0.04, 0.06 and 0.08, with an aspect ratio (M) of 2, as shown in Figure 3.10. The results shows the increase in χ_e/χ_m with increasing χ_r. When the nonlinear contrast is $\chi_r = 1$ or $\chi_i = \chi_m$, it gives $\chi_e/\chi_m = 1$, as expected. For $\chi_r > 1$, increasing the volume packing fraction v_i having χ_i more than χ_m, enhance the effective nonlinear coefficient (χ_e) of the composite. In contrast, for $\chi_r < 1$, increasing v_i having χ_i less than χ_m, reduces χ_e.

To determine the effects of inclusion shapes on χ_e, we report the variation of inclusion shapes by varying the nonlinear contrast (χ_r) upon the relative effective nonlinear coefficients (χ_e/χ_m), with the aspect ratios (M) = 1, 2, 3 and 10, as parameter, on a logarithmic scale in Figure 3.11 for an inclusion packing fraction (v_i) of 0.08. The results show the increase in χ_e/χ_m with increasing M within the range of $log(\chi_r) > 0.4$ (or $\chi_r \gg 2.5$). On the other hand, within the range of $log(\chi_r) < -0.4$ (or $\chi_r \ll 0.4$), increasing M reduces the effective nonlinear coefficient χ_e of the composite. For χ_i close to χ_m, or low nonlinear contrast range ($-0.4 \leq log(\chi_r) \leq 0.4$ or $0.4 \leq \chi_r \leq 2.5$), varying the aspect ratio rarely affects χ_e/χ_m of the composites for aspect ratios (M) within the evaluated range of M from 1 to 10.

In order to confirm the validity of the simple decoupling approximation, we consider the case of $M = 1$ that is cylindrical inclusion shape. Our results determined by using the simple decoupling approximation are compared with those

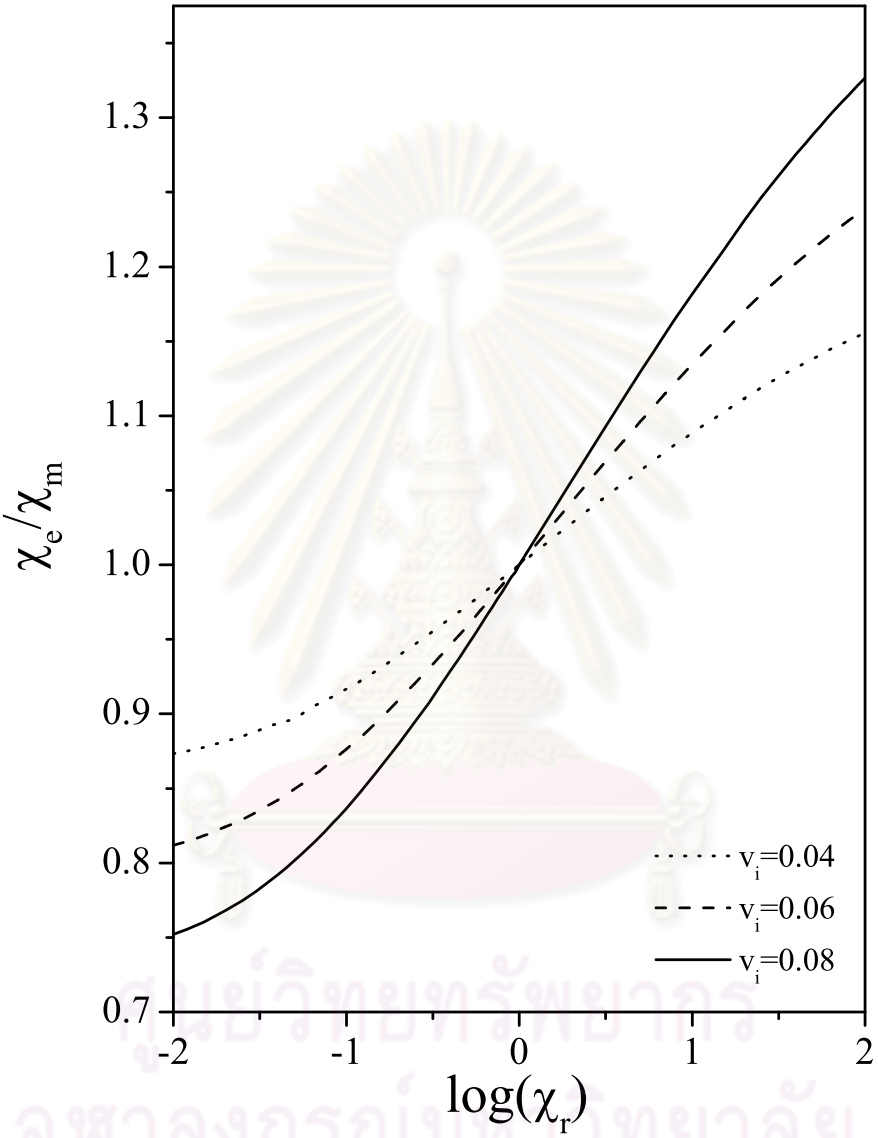

Figure 3.10: The relative effective nonlinear coefficients (χ_e/χ_m), with varying inclusion packing fractions (v_i) of 0.04, 0.06 and 0.08, and an aspect ratio (M) of 2 [21].

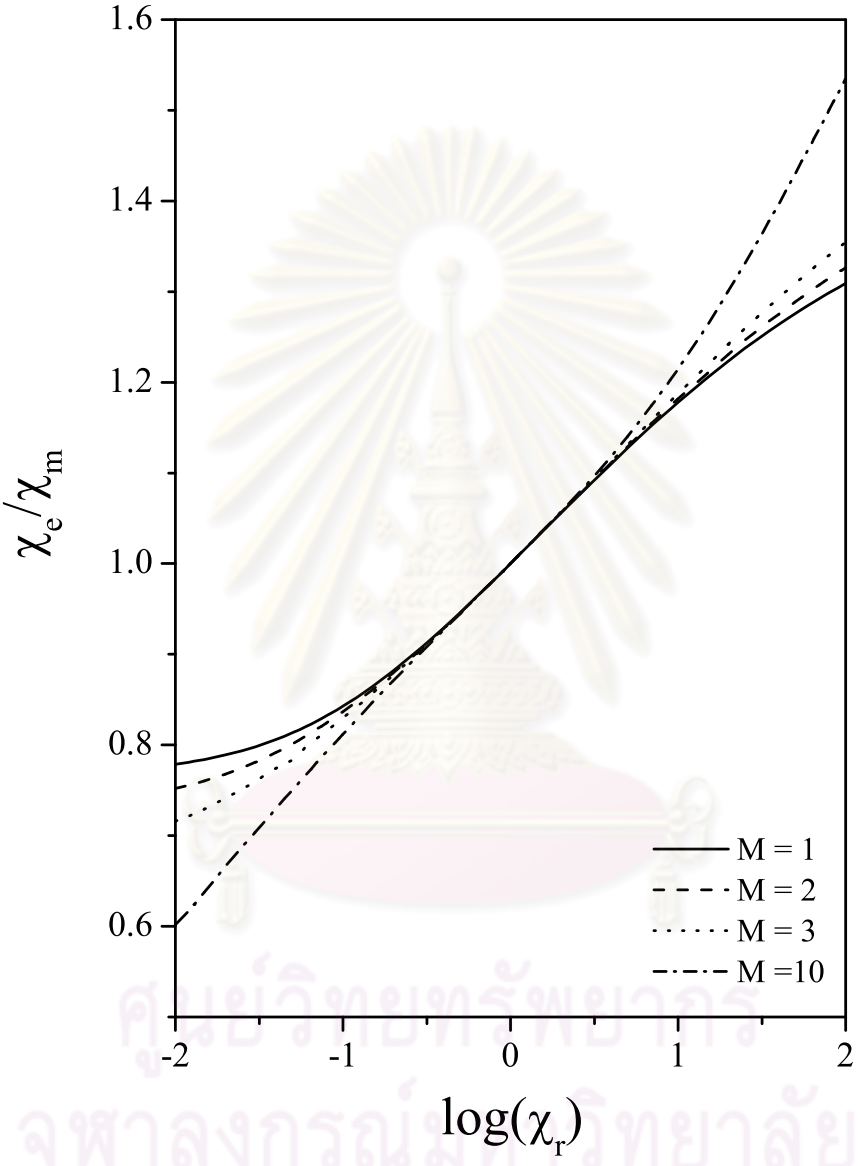

Figure 3.11: The relative effective nonlinear coefficients (χ_e/χ_m), with varying aspect ratios (M) between 1 and 10, and with an inclusion packing fraction (v_i) of 0.08 [21].

determined using the simple variational method of Yu and Gu [8], as shown in Figure 3.12. A good agreement between the two methods throughout was observed and the discussion was reported in reference [21].

We also estimated the validity of χ_e by considering the simple decoupling approximation used in the derivation of the effective nonlinear coefficients (χ_e), where we approximate $\langle E_m^4 \rangle \approx \langle E_m^2 \rangle^2$. Because the electric field inside the inclusion is exact, it gives $\langle E_i^4 \rangle = \langle E_i^2 \rangle^2$. Therefore, we considered the validity of approximation $\langle E_m^4 \rangle \approx \langle E_m^2 \rangle^2$ as a percentage of discrepancy ($\Delta\%$). The percentage of discrepancy ($\Delta\%$) is evaluated from $\Delta\% = [\langle E_m^4 \rangle - \langle E_m^2 \rangle^2) / \langle E_m^4 \rangle] \times 100$ by using the electric fields from the variational method. Figure 3.13 shows the percentage discrepancy ($\Delta\%$) used in the decoupling approximation with an aspect ratio (M) = 1 and inclusion packing fractions (v_i) of 0.04, 0.06 and 0.08. The percentage of discrepancy reveals that χ_e are reliable within the illustrated range of χ_r and v_i. The discussion of $\Delta\%$ was reported in reference [21].

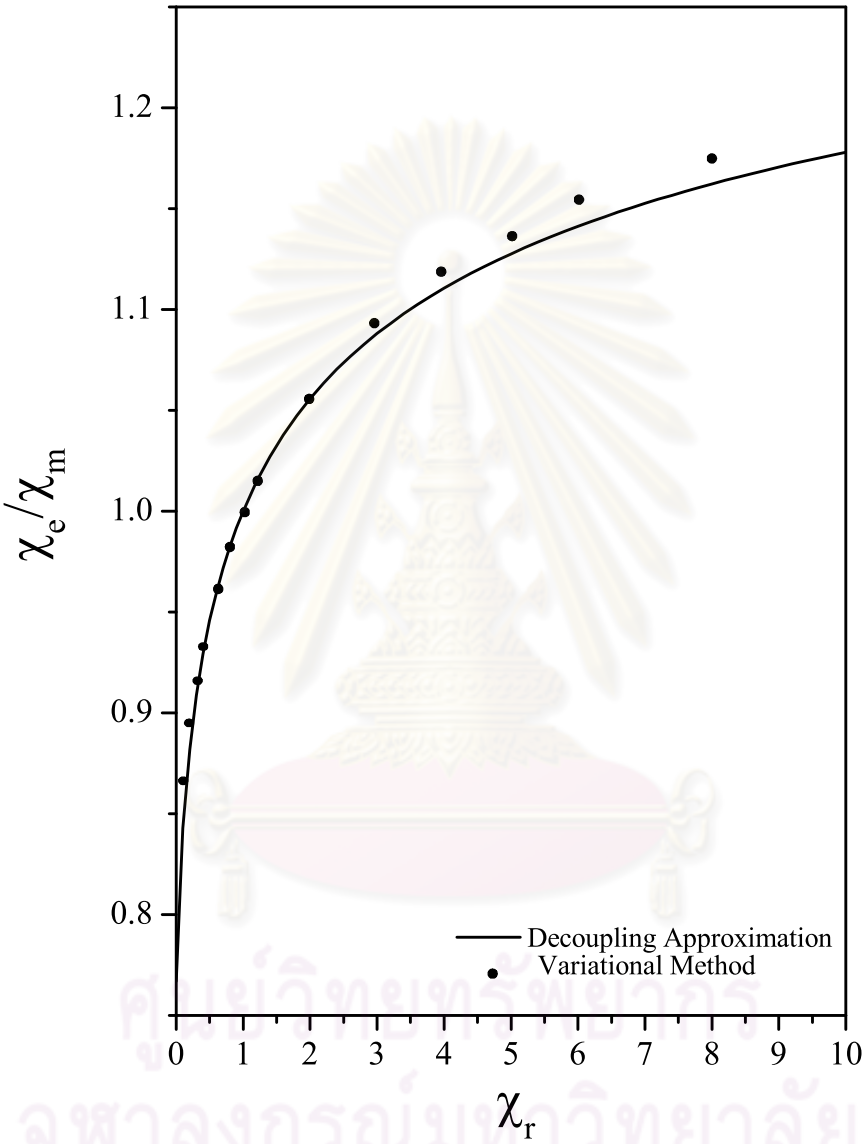

Figure 3.12: Comparison of the relative effective nonlinear coefficients (χ_e/χ_m) obtained from the decoupling approximation and the variational method for an aspect ratio (M)) of 1 and an inclusion packing fraction (v_i) of 0.08 [21].

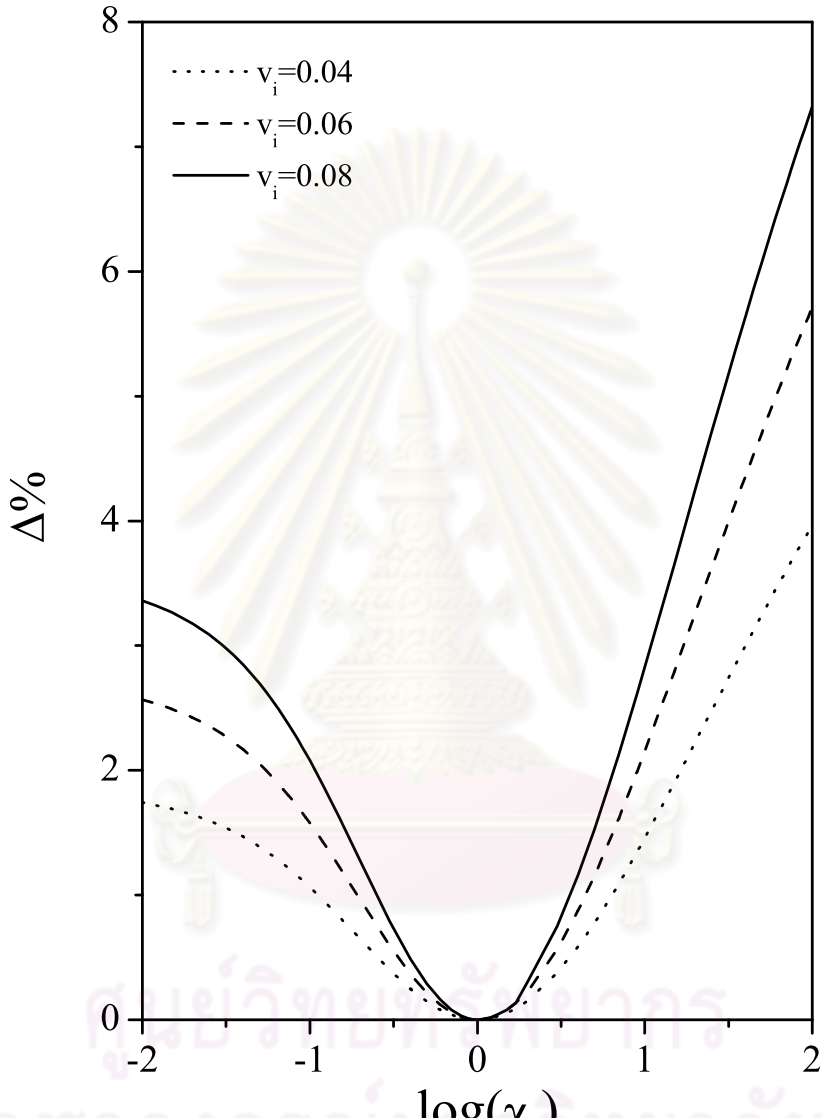

Figure 3.13: The percentage discrepancy ($\Delta\%$) between $\langle E_m^4 \rangle$ and $\langle E_m^2 \rangle^2$ used in the decoupling approximation with an aspect ratio (M) of 1 and inclusion packing fractions (v_i) of 0.04, 0.06 and 0.08 [21].

CHAPTER IV

Composites with Distributed Inclusion Shapes

In this chapter, we concentrate on elliptic cylindrical dielectric composites with distributed inclusion shapes in two dimensions. The composites consist of elliptic cylindrical inclusions, having the variation in shape and the random orientation, which are embedded in a different dielectric media in the dilute limit. The relation between the electric displacement ($\mathbf{D}$) and electric field ($\mathbf{E}$) of the inclusions has the form $\mathbf{D} = \varepsilon\mathbf{E} + \chi|\mathbf{E}|^{\beta}\mathbf{E}$ where β is a nonlinear integer exponent for weakly nonlinear composites. For strongly nonlinear composites, the dielectric property of both inclusion and medium satisfying $\mathbf{D} = \chi|\mathbf{E}|^{2}\mathbf{E}$ is considered. In this research, three types of the composites, linear, weakly nonlinear and strongly nonlinear are considered. Firstly, the effective linear coefficient (ε_e) of linear elliptic cylindrical composite is determined. Secondly, a brief review of the statistical approach proposed by Goncharenko [22] is presented. Thirdly, it is applied to determine the effective nonlinear coefficients (χ_e) of weakly and strongly nonlinear composites with the same microstructure as a linear composite by using the decoupling approximation. We also determine χ_e directly without the decoupling approximation for $\beta = 2$ in order to confirm the results. Finally, our results χ_e are reported including with the effects of inclusion shapes on χ_e to be predicted.

4.1 Linear Dielectric Composites

4.1.1 Typical Structure and Model

We consider a linear composite with distributed inclusion shapes, which composes of variation in shape of elliptic cylindrical inclusions of the volume packing fractions v_i, randomly oriented and embedded in a different linear dielectric medium of the volume packing fraction $v_m = 1 - v_i$. The linear coefficients of the inclusions and the host medium are ε_i and ε_m, respectively. Figure 4.1 shows a linear dielectric composite with distributed inclusion shapes.

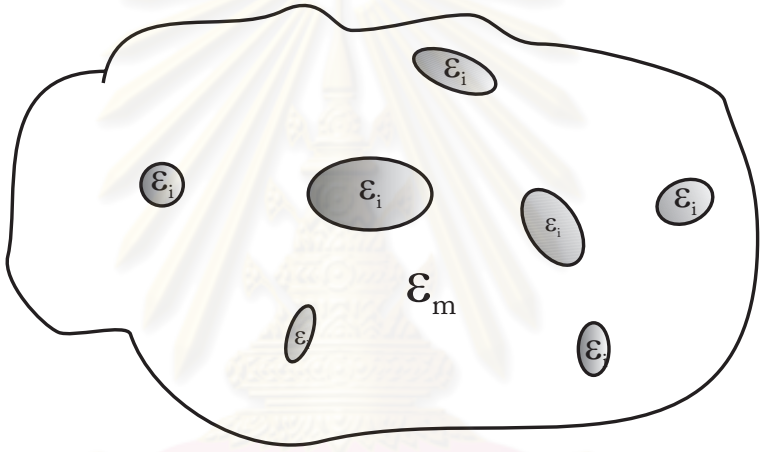

Figure 4.1: A linear dielectric composite with distributed inclusion shapes.

In the dilute limit, the single inclusion model is assumed. The external electric field is applied as shown in Figure 4.2,

$$\mathbf{E}_0 = E_0 \cos(\alpha)\hat{x} + E_0 \sin(\alpha)\hat{y}, \tag{4.1}$$

where α is the angle between $\mathbf{E}_0$ and the major axis of the inclusion aligned in the $\widehat{x}$ direction. We have to determine the electric field inside the elliptic cylindrical inclusion as shown in Figure 4.2.

4.1.2 Electric Field inside an Elliptic Cylindrical Inclusion

The electric field inside an ellipsoidal inclusion was solved by Stratton [39] in 1941, and Landau and Lifshitz [40] in 1960. These are widely applied as a

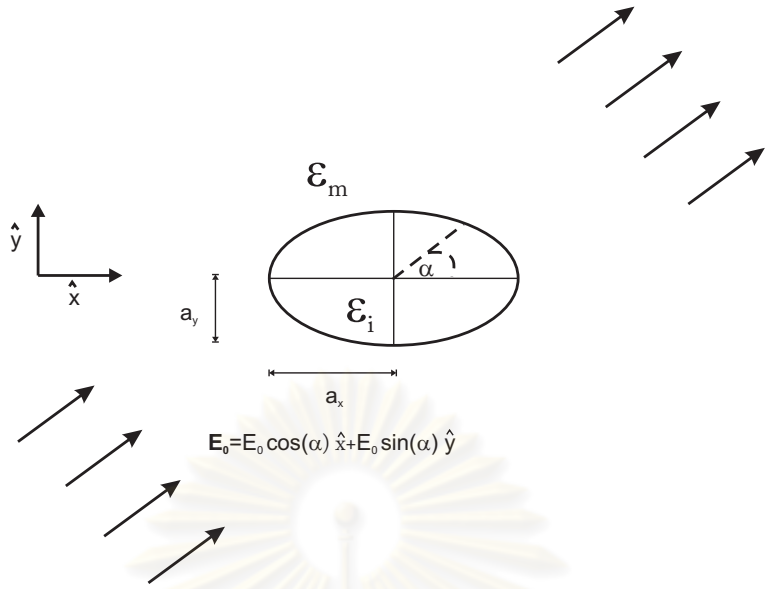

Figure 4.2: The single inclusion model for a composite with distributed inclusion shapes.

basis in the studying of the effective linear and nonlinear responses of ellipsoidal composites and related fields by many authors such as Yu et al. [4] and Giordano [18]. Giordano used the effective medium theory to investigate the shape effect of inclusion on effective linear response of ellipsoidal dielectric composites. The electric field inside the ellipsoidal inclusion was calculated, and then the explicit formula of effective linear coefficient (ε_e) was determined by using the differential method in terms of eccentricity. In this research, we follow Giordano 's work to determine the effective linear coefficient of elliptic cylindrical composites.

Generally, let a uniform electric field ($\mathbf{E}_0$) be applied to an elliptic cylindrical inclusion, which has the axes a_x and a_y aligned in the x and y components, respectively, as shown in Figure 4.2. The electric field inside inclusion induced by the external uniform electric field can be written as

$$\mathbf{E}_i = \beta_x E_{0x}\hat{x} + \beta_y E_{0y}\hat{y}. \tag{4.2}$$

β_j is the field factor ($j = x$ or y) proposed by Stratton [39], and Landau and Lifshitz [40], which can be expressed by

$$\beta_j = \frac{\varepsilon_m}{\varepsilon_m + L_j(\varepsilon_i - \varepsilon_m)}, \tag{4.3}$$

where L_j is the depolarization factor (the ratio of the internal electric field induced by the charges on the surface of a dielectric when an external electric field is applied to the polarization of the dielectric). Generally, L_j depends on the inclusion shape and is restricted by $L_x + L_y = 1$. The depolarization factor of an elliptic cylindrical inclusion depends on its shape by [18]

$$L_j = \frac{a_x a_y}{2} \int_0^\infty \frac{du}{(u + a_j^2)\sqrt{(u + a_x^2)(u + a_y^2)}}, \tag{4.4}$$

where a_j is the the axe of elliptic cylinder aligned along j direction. For the system considered here, the electric field inside the elliptic cylindrical inclusion can written as the superposition of the responses in $\hat{x}$ and $\hat{y}$ directions according to equation (4.2) by

$$\mathbf{E}_i = \beta_x E_0 \cos(\alpha)\hat{x} + \beta_x E_0 \sin(\alpha)\hat{y}. \tag{4.5}$$

This is an important equation to be used to calculate the effective linear coefficient (ε_e) by using the average field method in the next section.

4.1.3 Effective Linear Coefficient

By using the average field method as briefly described in section 3.1.3, the effective linear coefficient is therefore determined by

$$\varepsilon_e = \varepsilon_m + \frac{(\varepsilon_i - \varepsilon_m)}{V E_0^2} \mathbf{E}_0 \cdot \int_{V_i} \mathbf{E}_i dV. \tag{4.6}$$

Replacing $\mathbf{E}_0 = E_0 \cos(\alpha)\widehat{x} + E_0 \sin(\alpha)\widehat{y}$ and $\mathbf{E}_i$ from Eq. (4.5) into (4.6), it leads to

$$\varepsilon_e^\alpha = \varepsilon_m + v_i(\varepsilon_i - \varepsilon_m)\left[\beta_x \cos^2\alpha + \beta_y \sin^2\alpha\right]. \tag{4.7}$$

For totally randomly oriented elliptical inclusions, we take the angular average over angle α to Eq. (4.7) with the integral

$$\varepsilon_e = \frac{1}{2\pi} \int_0^{2\pi} \varepsilon_e^\alpha d\alpha. \tag{4.8}$$

We obtain

$$\varepsilon_e = \varepsilon_m + \frac{v_i}{2}(\varepsilon_i - \varepsilon_m)\left[\beta_x + \beta_y\right]. \tag{4.9}$$

Substituting the expression of β_x and β_y given by Eq. (4.3) into Eq. (4.9) and using the relation $L_y = 1 - L_x$, we obtain the effective linear coefficient (ε_e) in terms of the depolarization factor L_x as

$$\varepsilon_e = \varepsilon_m \left[1 + \frac{v_i(\varepsilon_i - \varepsilon_m)}{2} \left(\frac{1}{\varepsilon_m + L_x(\varepsilon_i - \varepsilon_m)} + \frac{1}{\varepsilon_m + (1 - L_x)(\varepsilon_i - \varepsilon_m)} \right) \right]. \tag{4.10}$$

For convenience in calculation, we take $L_x = L$ to Eq. (4.10) and obtain

$$\varepsilon_e = \varepsilon_m \left[1 + \frac{v_i(\varepsilon_i - \varepsilon_m)}{2} \left(\frac{1}{\varepsilon_m + L(\varepsilon_i - \varepsilon_m)} + \frac{1}{\varepsilon_m + (1 - L)(\varepsilon_i - \varepsilon_m)} \right) \right]. \tag{4.11}$$

We note that inclusions are still identical shape. For cylindrical inclusions, the depolarization factors are $L = L_x = L_y = 1/2$ ($L_z = 0$). Eq. (4.11) leads to the well-known result of a linear cylindrical dielectric composite in the dilute limit of $\varepsilon_e = \varepsilon_m \left[1 + 2v_i \frac{(\varepsilon_i - \varepsilon_m)}{(\varepsilon_i + \varepsilon_m)} \right]$, as expected.

For the composite with the elliptic cylindrical inclusions having different shapes (or distributed inclusion shapes), the effective linear coefficient (ε_e) is related to the effective linear coefficient of the equivalent composite with identical inclusion shape ($\varepsilon_e^{identical}$) based on the statistical approach by [22]

$$\varepsilon_e = \int \varepsilon_e^{identical} P(L) dL, \tag{4.12}$$

where $P(L)$ is shape distribution function. $P(L)dL$ is the probability for an inclusion to have the depolarization factor L lying within the range between L and $L + dL$. The shape distribution function is considered to be normalized to unity:

$$\int P(L) dL = 1. \tag{4.13}$$

The form of $P(L)$ has been assumed as [27]

$$P(L) = \frac{1}{\Delta} \theta \left(L - \frac{1}{2} + \frac{1}{2}\Delta \right) \theta \left(\frac{1}{2} + \frac{1}{2}\Delta - L \right), \tag{4.14}$$

where Δ is the shape distribution parameter and θ is the heaviside function. Generally, Δ can vary from zero, which all inclusions are cylindrical in shape, to unity, which any shapes of elliptic cylindrical inclusions are equiprobable. Alternative distribution such as the gamma distribution [41], binary distribution [42] and log-normal distribution [42] can be treated similarly. However, $P(L)$ given by Eq.

(4.14) yields the appropriate results of ε_e very close to that of realistic composites [22, 26].

By using Eqs. (4.11) - (4.14), we obtain the effective linear coefficient (ε_e) of composite with distributed inclusion shapes

$$\varepsilon_e = \varepsilon_m \left(1 + \frac{v_i}{\Delta} ln \left[\frac{(1+\Delta)\varepsilon_i + (1-\Delta)\varepsilon_m}{(1-\Delta)\varepsilon_i + (1+\Delta)\varepsilon_m}\right]\right). \tag{4.15}$$

Moreover, for $\Delta \to 0$, all inclusions are cylindrical in shape. Eq. (4.15) is reduced to the familiar result of a linear cylindrical dielectric composite in the dilute limit of $\varepsilon_e = \varepsilon_m \left[1 + 2v_i \frac{(\varepsilon_i - \varepsilon_m)}{(\varepsilon_i + \varepsilon_m)}\right]$, as expected. Because of the same basic field equations of both the dielectric without free charge and the conductor without free current, Eq. (4.15) is also consistent with Eq. (17) reported by Gao et al. [27] for the effective conductivity of the equivalent composite structure with shape distribution in the dilute limit.

4.1.4 Results and Discussion

In Figure 4.3, the relative effective linear coefficients ($\varepsilon_e/\varepsilon_m$) are reported on the logarithmic scale for varying the contrast (ε_r) within the range from 0.001 to 1000 with the depolarization factor (L) as parameter and the inclusion packing fraction (v_i) of 0.08. The results show the increase in $\varepsilon_e/\varepsilon_m$ with increasing the depolarization factor (L) within the range of $log(\varepsilon_r) > 0.3$ (or $\varepsilon_r \gg 2.0$). In contrast, within the range of $log(\varepsilon_r) < -0.3$ (or $\varepsilon_r \ll 0.5$), increasing the depolarization factor(L) reduces the effective linear coefficient ε_e. For small contrast of ε_r, increasing the depolarization factor(L) rarely affect ε_e of linear elliptic cylindrical composite with distributed inclusion shapes. These ranges of ε_r agree with those in Figure 3.4, which are analyzed in terms of the aspect ratio (M) but now ε_r are analyzed in terms of the depolarization factor (L), as expected. In comparison between Figure 4.3 and Figure 3.4, the inclusion shapes such as the aspect ratio (M) and the depolarization factor (L) rarely affect ε_e within the range of $-0.3 \leq log(\varepsilon_r) \leq 0.3$ or $05 \leq \varepsilon_r \leq 2.0$.

For $\varepsilon_r > 1$, Figure 4.4 shows the relative effective linear coefficients ($\varepsilon_e/\varepsilon_m$) for varying the depolarization factor (L) with the contrast (ε_r) as parameters for

inclusion packing fraction (v_i) of 0.08. The results reveal the rapid increase in (χ_e/χ_i) with increasing ε_r for $L < 0.3$ and $L > 0.7$. Physically, the deviation of inclusions from cylinder to elliptic cylinder in this range affects the rapid increase in ε_e. In contrast, increasing the depolarization factor within the range of $0.3 \leq L \leq 0.7$ rarely affects ε_e of composites.

Moreover, for $L = 0.5$, the inclusions are circular cylinders or rods. The results of ε_e show the symmetry around $L = 0.5$. This symmetry is observed because of the restriction of $L_x + L_y = 1$. In addition, the results of ε_e concur with those reported in Figure 4.4 for $M = 1$ throughout.

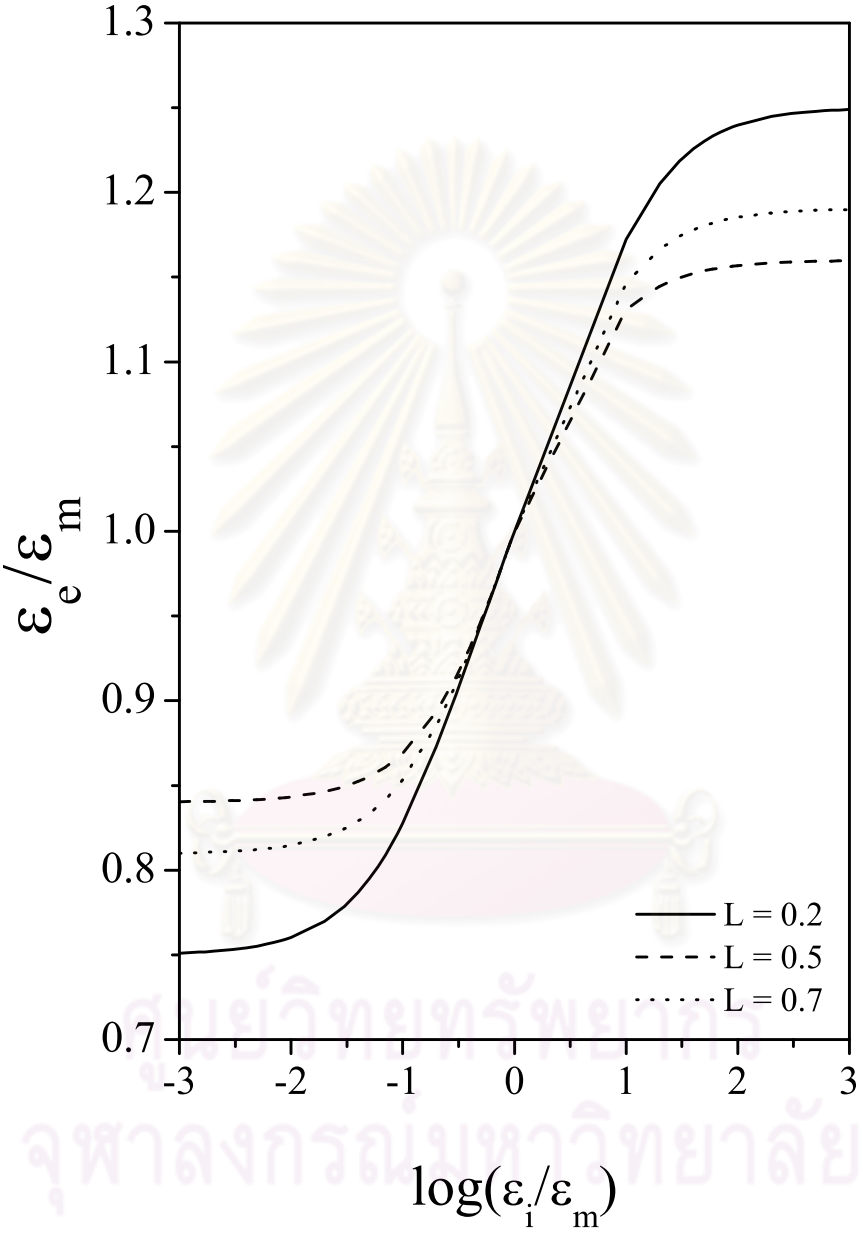

Figure 4.3: The relative effective linear coefficients ($\varepsilon_e/\varepsilon_m$) for varying the contrast (ε_r) with the depolarization factor (L) as parameter for inclusion packing fraction (v_i) of 0.08.

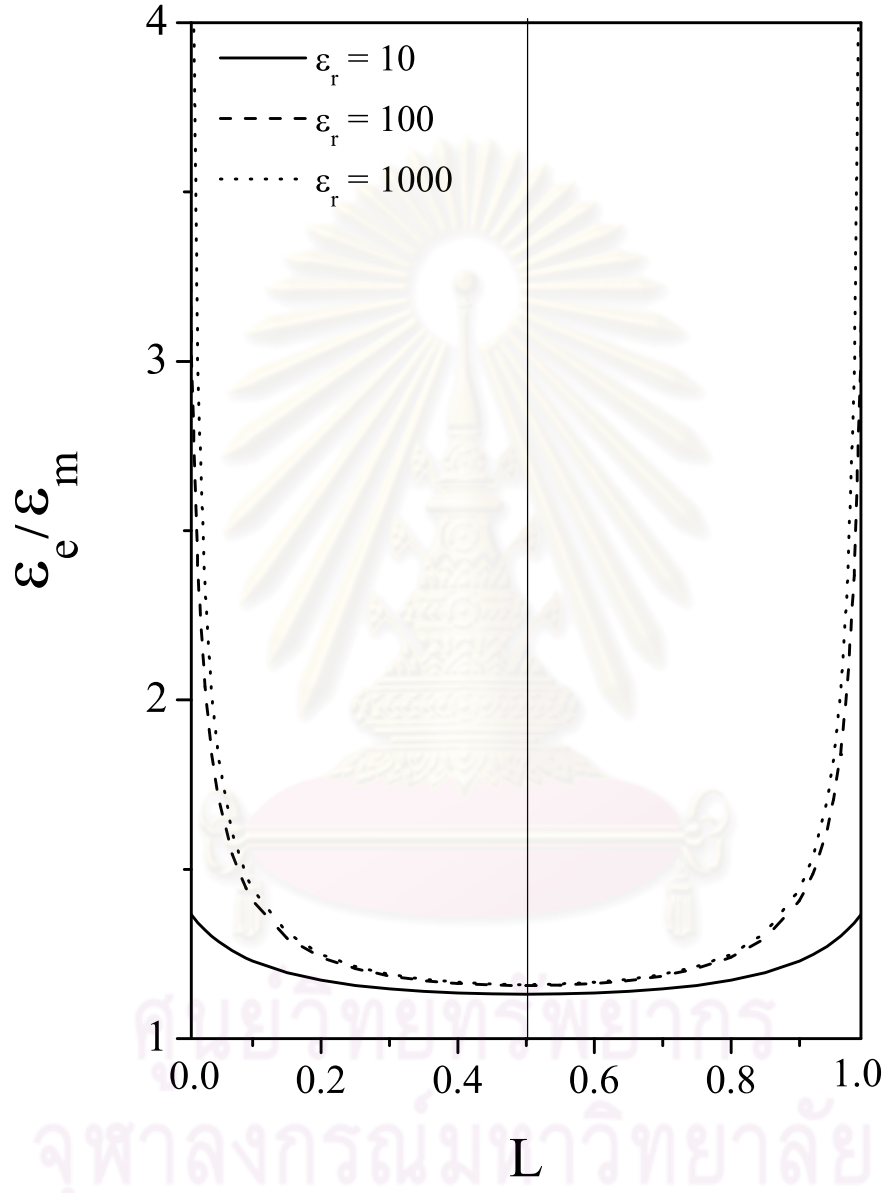

Figure 4.4: The relative effective linear coefficients ($\varepsilon_e/\varepsilon_m$) for varying the depolarization factor (L) with the contrast (ε_r) as parameter for inclusion packing fraction (v_i) of 0.08.

For linear composite with distributed inclusion shapes, in Figure 4.5, the relative effective linear coefficients ($\varepsilon_e/\varepsilon_m$) are reported on the logarithmic scale for varying the linear contrast (ε_r) within the range from 0.001 to 1000 with the shape distribution parameter (Δ) as parameter and the inclusion packing fraction (v_i) of 0.08. The results show the monotonically increase in $\varepsilon_e/\varepsilon_m$ with increasing ε_r. For small ε_r, $-0.3 \leq log(\varepsilon_r) \leq 0.3$ (or $0.5 \leq \varepsilon_r \leq 2.0$), increasing Δ from 0 to 1 slightly affects on $\varepsilon_e/\varepsilon_m$. Therefore, the shape distribution parameter describing the variation in shape of inclusions, rarely affects on ε_e in this range of ε_r. However, for large ε_r, $log(\varepsilon_r) < -0.3$ (or < 0.5) and $log(\varepsilon_r) > 0.3$ (or $\varepsilon_r > 2.0$), Δ directly affects on ε_e. For $\Delta = 1$, ε_e linearly increases with increasing Δ so ε_e have less dependent on ε_r as Δ near 1.

Figure 4.6 shows the relative effective linear coefficients ($\varepsilon_e/\varepsilon_m$) for varying the shape distribution parameter with the linear contrast (ε_r) as parameters a) $\varepsilon_r < 1$ and b) $\varepsilon_r > 1$. In Figure 4.6 a), the results show that $\varepsilon_e/\varepsilon_m$ monotonically decreases with increasing Δ. However, for $\varepsilon_r > 1$ in Figure 4.6 b), $\varepsilon_e/\varepsilon_m$ monotonically increases with increasing Δ. For small Δ, $0 \leq \Delta \leq 0.6$, increasing Δ rarely affects ε_e. In contrast, for high Δ, $0.6 < \Delta \leq 1.0$, increasing Δ affects rapid increase in ε_e.

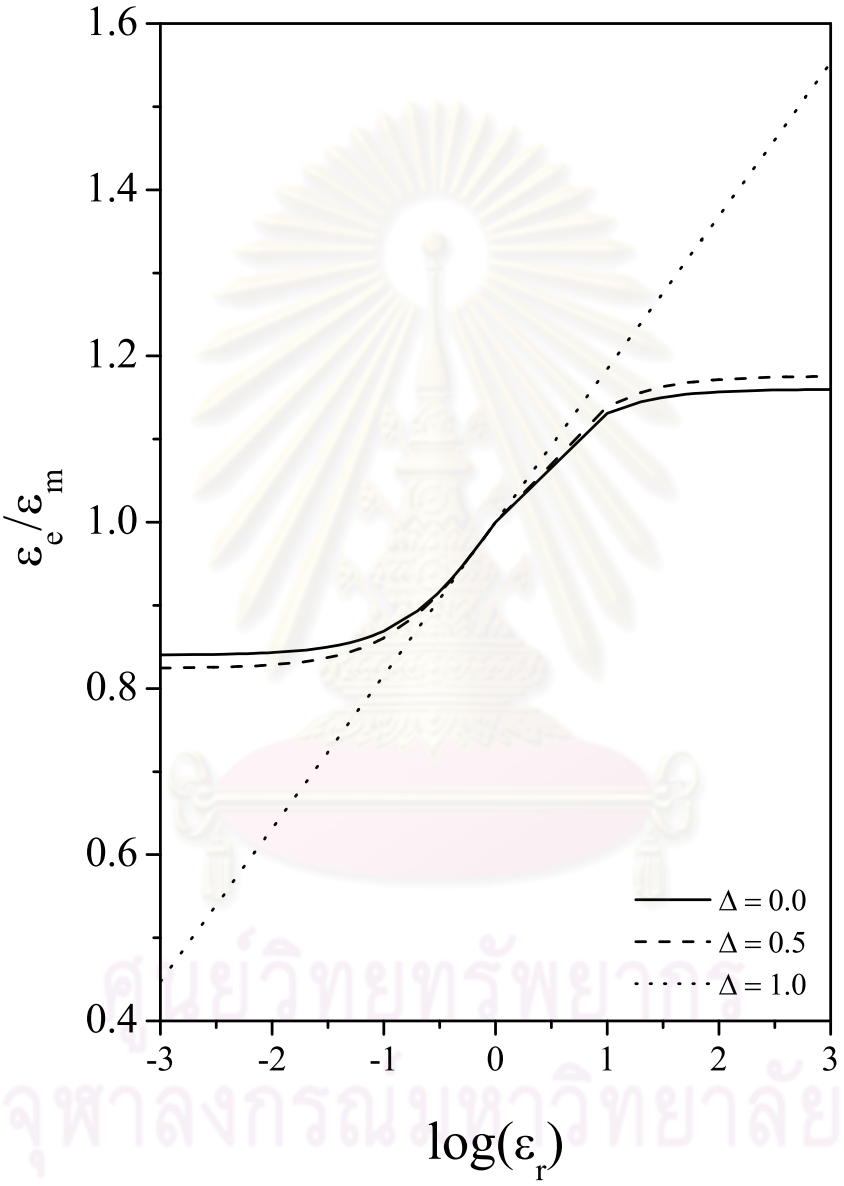

Figure 4.5: The relative effective linear coefficients ($\varepsilon_e/\varepsilon_m$) for varying the linear contrast (ε_r) with the shape distribution parameter as parameter.

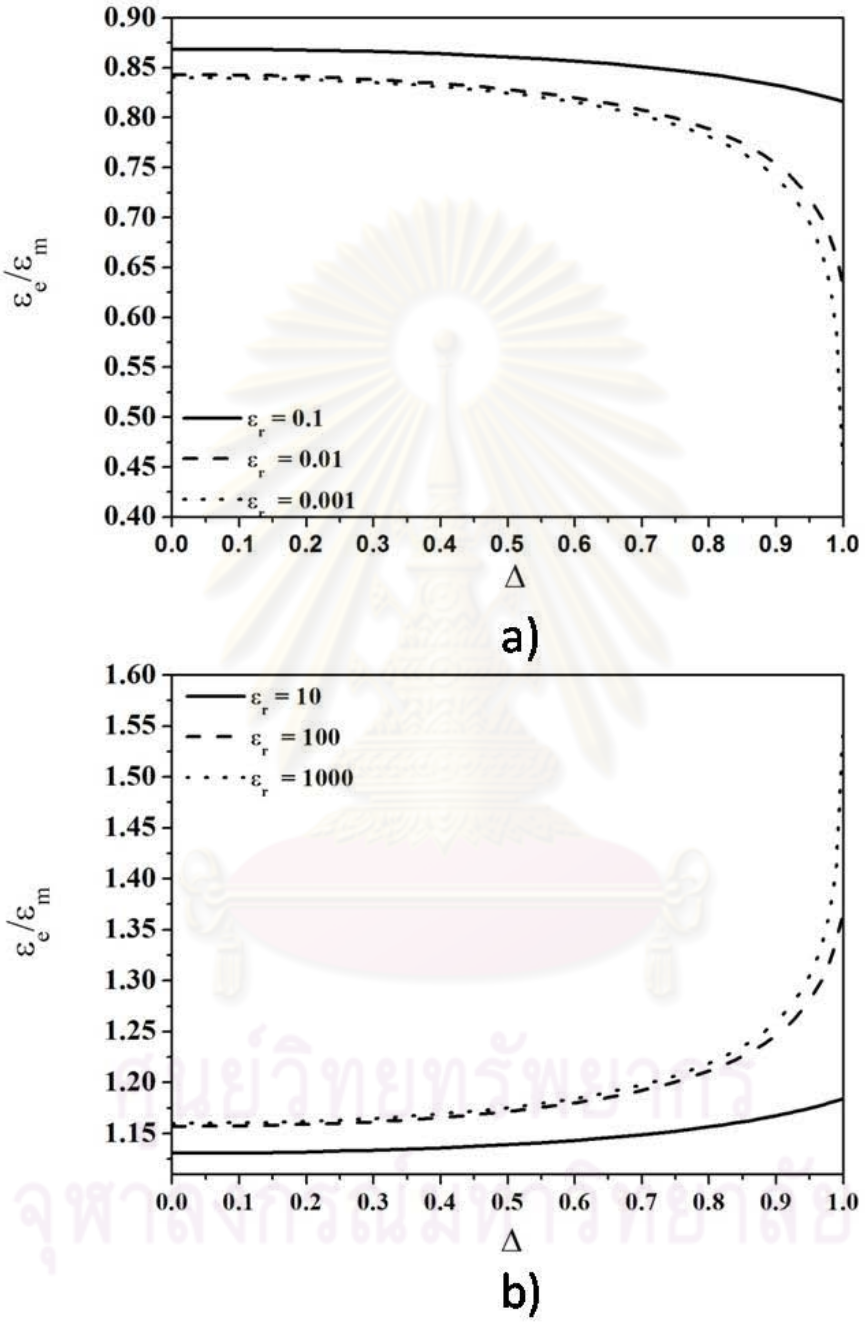

Figure 4.6: The relative effective linear coefficients ($\varepsilon_e/\varepsilon_m$) for varying the the shape distribution parameter with the linear contrast (ε_r) as parameter.

4.2 Weakly Nonlinear Dielectric Composite

4.2.1 Typical Structure

We now consider a nonlinear composite with distributed inclusion shapes in two dimensions, which have the same microstructure as a linear dielectric composite described previously. The composite consists of nonlinear elliptic cylindrical inclusions with distributed shapes randomly oriented and embedded in a linear dielectric medium in dilute limit, as shown in Figure 4.7. The relation between the electric displacement ($\mathbf{D}$) and electric field ($\mathbf{E}$) inside the inclusions is $\mathbf{D} = \varepsilon\mathbf{E} + \chi|\mathbf{E}|^{\beta}\mathbf{E}$ with $\chi|\mathbf{E}|^{\beta} \ll \varepsilon$. The linear and nonlinear coefficients of inclusions and medium are ε_i, χ_i and ε_m, $\chi_m = 0$, respectively.

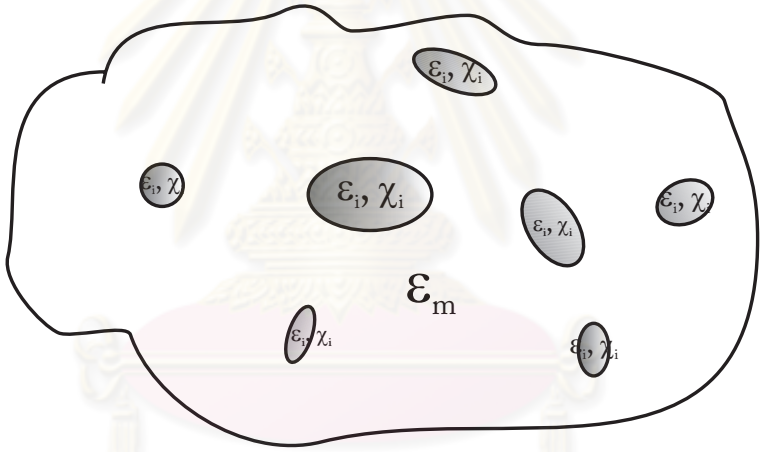

Figure 4.7: A nonlinear dielectric composite with distributed inclusion shapes.

4.2.2 Effective Nonlinear Coefficient

Simple Decoupling Approximation

In case of weakly nonlinear dielectric composite, the nonlinear response is small compared to the linear response. We follow the work of Hui and Chung [11] which has the same basic relation between the electric displacement ($\mathbf{D}$) and electric field ($\mathbf{E}$) as this thesis. The effective nonlinear coefficient (χ_e) can be

defined by using the average energy method. The energy of effective medium is defined by $W = \int \mathbf{D} \cdot \mathbf{E} dV$, which equals the sum of the energy of the inclusion and medium. The effective nonlinear coefficient (χ_e) can be expressed as [11]

$$\begin{aligned} \chi_e &= \frac{1}{V E_0^{\beta+2}} \left(\int_{V_i} \chi_i |\widetilde{E}_i|^{\beta+2} dV + \int_{V_m} \chi_m |\widetilde{E}_m|^{\beta+2} dV \right), \\ &= \frac{1}{E_0^{\beta+2}} \left(v_i \chi_i \langle \widetilde{E}_i^{\beta+2} \rangle + v_m \chi_m \langle \widetilde{E}_m^{\beta+2} \rangle \right), \end{aligned} \tag{4.16}$$

where $\widetilde{E}_i$ and $\widetilde{E}_m$ are the nonlinear electric fields inside the inclusions and medium, respectively.

By using the simple decoupling approximation, the nonlinear electric fields of $\widetilde{E}_i$ and $\widetilde{E}_m$ required Eq. (4.16) are approximated to be linear field E_i and E_m. The expressions of χ_e becomes

$$\chi_e = \frac{1}{E_0^{\beta+2}} \left(v_i \chi_i \langle E_i^{\beta+2} \rangle + v_m \chi_m \langle E_m^{\beta+2} \rangle \right). \tag{4.17}$$

For our case ($\chi_m = 0$), the effective nonlinear coefficient (χ_e) is

$$\chi_e = \frac{1}{E_0^{\beta+2}} \left(v_i \chi_i \langle E_i^{\beta+2} \rangle \right), \tag{4.18}$$

where $\left\langle E_i^{\beta+2} \right\rangle = (1/V_i) \int_{V_i} |\mathbf{E}_i|^{\beta+2} dV$, E_i is the linear electric fields and v_i is the inclusion volume packing fractions.

For distributed inclusion shapes, Goncharenko et al. [22-23] successfully predicted the effect of shape distribution on light absorption and light scattering of ellipsoidal composites by using statistical approach. Their work has been widely applied to composite with distributed inclusions shapes in various field of physics [24-32] such as the work of Gao et al. [27]. In their work, the effective nonlinear response of a two components in two dimensions of strongly nonlinear composite media in which one component possesses a shape distribution is investigated. The inclusions are considered to be elliptic cylinders with distributed inclusion shapes. Based on the statistical approach, the effective medium model and the decoupling approximation, the effective nonlinear coefficient (χ_e) of strongly nonlinear composite is determined for all concentrations of inclusion. In this section, we apply the statistical approach to elliptic cylindrical composite with distributed inclusion

shapes and then the effective nonlinear coefficient (χ_e) is determined by using the decoupling approximation.

Similar to the process in determination on ε_e in section 4.1.3, the effective nonlinear coefficient (χ_e) of composite with distributed inclusion shapes is related to the effective nonlinear coefficient of the equivalent composite with identical inclusion shape ($\chi_e^{identical}$) based on the statistical approach by [22]

$$\chi_e = \int \chi_e^{identical} P(L) dL, \tag{4.19}$$

By using the shape distribution function $P(L)$ given by Eq. (4.14) and the expression of χ_e given by Eq. (4.18), the effective nonlinear coefficient of composite with distributed inclusion shapes (χ_e) from equation (4.19) is

$$\chi_e = \frac{v_i \chi_i}{E_0^{\beta+2}\Delta} \int_{\frac{1}{2}-\frac{1}{2}\Delta}^{\frac{1}{2}+\frac{1}{2}\Delta} \left\langle E_i^{\beta+2} \right\rangle dL. \tag{4.20}$$

We invoke the simple decoupling approximation which simplifies the calculation by

$$\langle E_i^{\beta+2} \rangle \approx \langle E_i^2 \rangle^{(\beta+2)/2}. \tag{4.21}$$

The replacement of Eq. (4.21) into Eq. (4.20) leads to the equation for determining χ_e;

$$\chi_e = \frac{v_i \chi_i}{E_0^{\beta+2}\Delta} \int_{\frac{1}{2}-\frac{1}{2}\Delta}^{\frac{1}{2}+\frac{1}{2}\Delta} \langle E_i^2 \rangle^{(\beta+2)/2} dL. \tag{4.22}$$

The volume average of electric fields to the second power in the inclusions $\langle E_i^2 \rangle$ is evaluated from the derivative of the effective linear coefficients given as [9]:

$$\left\langle E_i^2 \right\rangle = \frac{1}{v_i} \frac{\partial \varepsilon_e}{\partial \varepsilon_i} E_0^2. \tag{4.23}$$

From Eqs. (4.11) , (4.22) and (4.23), we obtain the new results of effective nonlinear coefficient ($\widetilde{\chi}_e$) in terms of v_i, ε_r, χ_i, β and Δ, as needed.

Direct Method

In order to confirm the effective nonlinear coefficient χ_e of the simple decoupling approximation determined in the previous section, we consider that composite for $\beta = 2$.

According to the equation for determining χ_e written in Eq. (4.20), we can determine $\left\langle E_i^{\beta+2} \right\rangle$ directly without using the simple decoupling approximation by

$$\widetilde{\chi}_e = \frac{v_i \chi_i}{E_0^4 \Delta} \int_{\frac{1}{2}-\frac{1}{2}\Delta}^{\frac{1}{2}+\frac{1}{2}\Delta} \langle E_i^4 \rangle dL, \tag{4.24}$$

where $\langle E_i^4 \rangle = (1/V_i) \int_{V_i} |\mathbf{E}_i|^4 dV$.

To calculate $\langle E_i^4 \rangle$, we consider the electric field inside the elliptic cylindrical inclusion given by Eq. (4.5) $\mathbf{E}_i^{\alpha} = \beta_x E_0 \cos(\alpha)\hat{x} + \beta_x E_0 \sin(\alpha)\hat{y}$. For totally randomly oriented elliptic cylindrical inclusions, the angular average of electric field inside the inclusion to the forth power ($|\mathbf{E}_i|^4$) is used:

$$\begin{aligned} |\mathbf{E}_i|^4 &= \frac{1}{2\pi} \int_0^{2\pi} |\mathbf{E}_i^{\alpha}|^4 \, d\alpha, \\ &= \frac{1}{4} \left[3\beta_x^4 + \beta_y^2 \beta_x^2 \right], \end{aligned} \tag{4.25}$$

where the field factors β_x and β_y are given by Eq. (4.3) for $j = x$ and y with the depolarization factor $L_y = 1 - L_x$. The volume integration of $|\mathbf{E}_i|^4$ yields $\langle E_i^4 \rangle$ as a function of L_x, which is replaced by L. Then we substitute the result of $\langle E_i^4 \rangle$ into Eq. (4.24). The effective nonlinear coefficient (χ_e) of elliptic cylindrical composite with distributed inclusion shapes is obtained as follows:

$$\chi_e = \frac{1}{2\Delta} v_i \chi_i \varepsilon_m^4 \left[\frac{\ln\left(\frac{A+\Delta B}{-A+\Delta B}\right)^2}{A^3 B} - \frac{32\Delta A^2}{C^3} - \frac{8\Delta}{C^2} - \frac{4\Delta}{A^2 C} \right], \tag{4.26}$$

where $A = \varepsilon_i + \varepsilon_m$, $B = \varepsilon_i - \varepsilon_m$ and $C = (\Delta^2 - 1)\varepsilon_i^2 - 2(\Delta^2 + 1)\varepsilon_i \varepsilon_m + (\Delta^2 - 1)\varepsilon_m^2$.

The closed form result of χ_e, as given by equation (4.26), is exact and firstly reported in this research.

4.2.3 Results and Discussion

For composites with distributed inclusion shapes, we obtain the relative effective nonlinear coefficient (χ_e/χ_i) with the nonlinear integer exponent (β) as parameter for an inclusion packing fraction $v_i = 0.08$ and the contrast a) $\varepsilon_r = 0.1$, b) $\varepsilon_r = 0.01$ and c) $\varepsilon_r = 0.001$, as shown in Figure 3.8 The results in Figure 3.8 a) reveal the rapidly increase in χ_e/χ_i with increasing Δ for $0.4 \leq \Delta \leq 1.0$ but for Δ less than 0.4, increasing the Δ slightly affect the increase in χ_e/χ_i. Similar behavior also perform with the enhancement of χ_e/χ_i for $\varepsilon_r = 0.01$ and 0.001, as reported in Figures 3.8 b) and c), respectively.

Figure 3.9 shows the relative effective nonlinear coefficient (χ_e/χ_i) for varying the contrast (ε_r) with the shape distribution parameter (Δ) equal to 0, 0.4 and 0.8 and the nonlinear integer exponents are a) $\beta = 2$, b) $\beta = 4$ and c) $\beta = 6$. For $\beta = 2$, the results reveal the increasing of χ_e/χ_i for decreasing ε_r which are more pronounced for larger values of Δ in the range of $0 \leq \varepsilon_r \leq 0.6$. On the other hand, for the contrast (ε_r) near 1 varying of Δ from 0 to 0.8 affects the slow increase in χ_e/χ_i. The similar analysis as for Figure 3.8 but now ε_e is from equation (4.11). Similar behaviors as seen in Figure 3.9 a) are also observed for $\beta = 4$ and $\beta = 6$ but the enhancement of χ_e/χ_i is much more pronounced for larger values of the nonlinear integer exponent (β).

Moreover, for $\beta = 2$, the exact values of χ_e/χ_i given by Eq. (4.26) obtained without using the decoupling approximation concur with the numerical values of those obtained by using the decoupling approximation throughout. For Δ approaches 0 which all inclusions are cylindrical shape, our results agree with those reported in Figure 3.8 a) for $M = 1$, as expected.

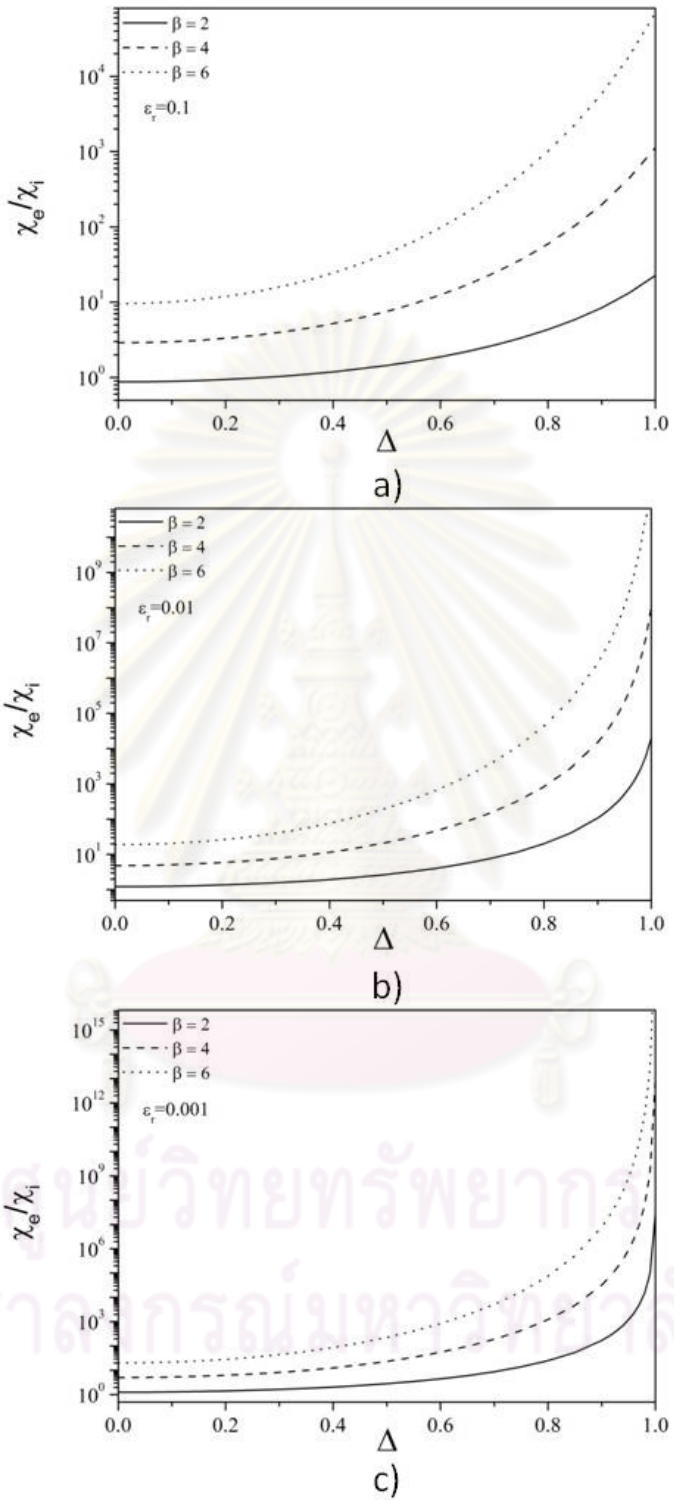

Figure 4.8: The relative effective nonlinear coefficient (χ_e/χ_i) for varying the shape distribution parameter (Δ) with the nonlinear integer exponent (β) equal to a) $\varepsilon_r = 0.1$, b) $\varepsilon_r = 0.01$ and c) $\varepsilon_r = 0.001$.

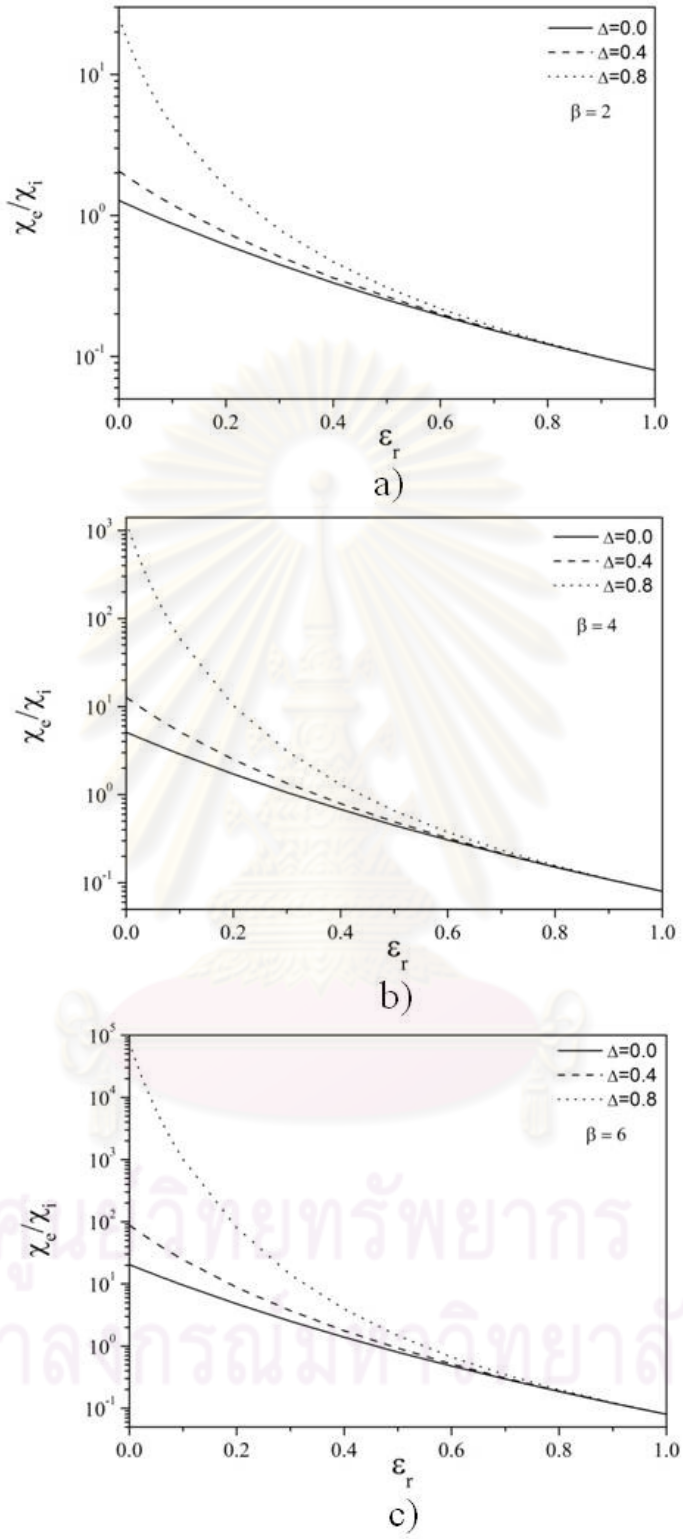

Figure 4.9: The relative effective nonlinear coefficients (χ_e/χ_i) for varying the contrast (ε_r) with the the nonlinear integer exponent (β) equal to a) $\beta = 2$, b) $\beta = 4$ and c) $\beta = 6$.

4.3 Strongly Nonlinear Dielectric Composite

In the literature search, the effective nonlinear response of a two-components strongly nonlinear elliptic cylindrical dielectric composite in which one component possesses a shape distribution was investigated by Gao et al. [27]. In their work, the numerical results of the effective nonlinear coefficient was determined for arbitrary inclusion packing fraction by using the effective medium approximation and the decoupling approximation, which includes the dilute limit expression. However, in such work does not discuss more information about the effect of inclusion shapes on χ_e. In order to obtain the information of inclusion shape effect on χ_e very close to realistic composite as possible, we further analyze that work in case of dilute limit. Moreover, the more information about the effect of inclusion shapes on χ_e have been discussed.

4.3.1 Typical Structure

We consider the strongly nonlinear elliptic cylindrical dielectric composite in two dimensions, which consists of variation in shape of elliptic cylindrical inclusions randomly oriented and embedded in a different dielectric medium in the dilute limit, as shown in Figure 4.10. It is assumed that the relationship between the electric displacement ($\mathbf{D}$) and the electric field ($\mathbf{E}$) for both inclusions and medium has the form $\mathbf{D} = \chi|\mathbf{E}|^2\mathbf{E}$ where $\varepsilon \ll \chi|\mathbf{E}|^2$ is of interest. The nonlinear coefficients of inclusion and medium are χ_i and χ_m

4.3.2 Effective Nonlinear Coefficient

We begin with a linear composite, which has the same microstructure as strongly nonlinear composite. The linear coefficients of the inclusions and the host medium are ε_i and ε_m, respectively. The average electric field inside the inclusion ($\overline{\mathbf{E}}_i$) subject to a uniform external field ($\mathbf{E}_0$) is assumed to be

$$\overline{\mathbf{E}}_i = \overline{\beta}\mathbf{E_0}, \tag{4.27}$$

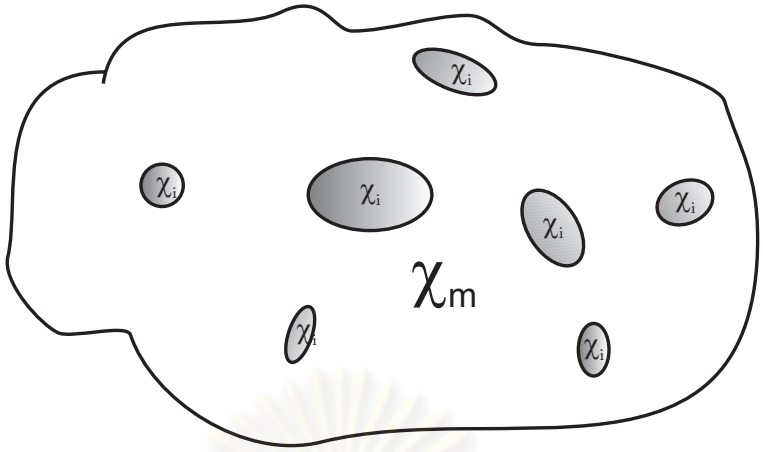

Figure 4.10: A strongly nonlinear dielectric composite with distributed inclusion shapes

where $\overline{\beta}$ is the average field factor.

Based on the statistical approach [22], the average field factor ($\overline{\beta}$) of composite with distributed inclusion shapes relates to the field factor of the equivalent composite but with identical inclusion shape (β) by

$$\overline{\beta} = \int \beta P(L) dL. \tag{4.28}$$

Substituting the the field factor (β) and the shape distribution parameter ($P(L)$), as given by Eqs. (4.3) and (4.14), respectively, including with the domain of integration $\frac{1}{2} - \frac{1}{2}\Delta < L < \frac{1}{2} + \frac{1}{2}\Delta$ as mention in section 3.2.2, the average field factor is [27]

$$\overline{\beta} = \frac{\varepsilon_m}{\Delta(\varepsilon_i + \varepsilon_m)} ln \left[\frac{(1+\Delta)\varepsilon_i + (1-\Delta)\varepsilon_m}{(1-\Delta)\varepsilon_i + (1+\Delta)\varepsilon_m} \right]. \tag{4.29}$$

Substituting $\overline{\beta}$ from Eq. (4.29) into Eq. (4.27) yields the electric field inside the inclusion as follow:

$$\overline{\mathbf{E}}_i = \frac{\varepsilon_m}{\Delta(\varepsilon_i + \varepsilon_m)} ln \left[\frac{(1+\Delta)\varepsilon_i + (1-\Delta)\varepsilon_m}{(1-\Delta)\varepsilon_i + (1+\Delta)\varepsilon_m} \right] E_0. \tag{4.30}$$

The average field method proposed by Landau and Lifshitz [40] is used with similar processes as proposed in Eq. (4.6). The effective linear coefficient (ε_e) for composite with distributed inclusion shapes is

$$\varepsilon_e = \varepsilon_m \left(1 + \frac{v_i}{\Delta} ln \left[\frac{(1+\Delta)\varepsilon_i + (1-\Delta)\varepsilon_m}{(1-\Delta)\varepsilon_i + (1+\Delta)\varepsilon_m} \right] \right). \tag{4.31}$$

Eq. (4.31) is consistent with Eq. (4.15), although the approaches of calculation are different. These confirm the result of ε_e.

The relations between the volume average of electric fields to the second power in the inclusions and host medium and the derivative of the effective linear coefficients are given as [9]:

$$\left\langle E_i^2 \right\rangle = \frac{1}{v_i} \frac{\partial \varepsilon_e}{\partial \varepsilon_i} E_0^2, \tag{4.32}$$

$$\left\langle E_m^2 \right\rangle = \frac{1}{v_m} \frac{\partial \varepsilon_e}{\partial \varepsilon_m} E_0^2, \tag{4.33}$$

where $\mathbf{E}_0$ is the external uniform electric field, and v_i and $v_m = 1 - v_i$ are the inclusion and medium volume fractions, respectively.

Substituting ε_e as given by Eq. (4.31) into Eqs. (4.32) and (4.33), we obtain the equations for determining $\langle E_i^2 \rangle$ and $\langle E_m^2 \rangle$ in terms of the shape distributed parameter (Δ), inclusion packing fraction (v_i), and the nonlinear contrast ($\chi_r = \chi_i/\chi_m$). By using the relations $\varepsilon_e = \chi_e E_0^2$, $\varepsilon_i = \chi_i \langle E_i^2 \rangle$ and $\varepsilon_m = \chi_m \langle E_m^2 \rangle$ [9], then $\langle E_i^2 \rangle$ and $\langle E_m^2 \rangle$ can be solved self-consistently depending on Δ, v_i and χ_r as parameters. The effective nonlinear coefficients (χ_e) of the composites can be determined from the relationship

$$\chi_e = \frac{v_i \chi_i \left\langle E_i^2 \right\rangle^2}{E_0^4} + \frac{v_m \chi_m \left\langle E_m^2 \right\rangle^2}{E_0^4}, \tag{4.34}$$

with the decoupling approximation, assuming that $\langle E_i^4 \rangle \approx \langle E_i^2 \rangle^2$ and $\langle E_m^4 \rangle \approx \langle E_m^2 \rangle^2$ [9].

4.3.3 Results and Discussion

By using the decoupling approximation, the effect of varying the nonlinear contrast between the nonlinear coefficients of inclusions and media (χ_r), with the shape distribution parameter (Δ) as parameter, upon the relative effective nonlinear coefficients (χ_e/χ_m) are shown on a logarithmic scale in Figure 4.11 for an inclusion packing fraction (v_i) of 0.08. Our results confirm the similar work of Gao et al. [27] which used the effective medium approximation in the dilute limit to predict the effective nonlinear coefficients (χ_e). The sigmoidal relationships shows the increase in χ_e/χ_m with increasing the shape distribution parameter within the range of $log(\chi_r) > 1$ (or $\chi_r \gg 10$) and that $\chi_e/\chi_m = 1$ when $\chi_r = 1$ or $\chi_i = \chi_m$. In contrast, within the range of $log(\chi_r) < 1$ (or $\chi_r \ll 0.1$), increasing the shape distribution parameter reduces the effective nonlinear coefficient χ_e of the composite. For small contrast, the results also show that increasing Δ rarely affect on χ_e of composites within the range of $-0.3 \leq log(\chi_r) \leq 0.5$ (or $0.5 \leq \chi_r \leq 3.2$). For higher contrast, within the range of $log(\chi_r) < -0.3$ (or $\chi_r \ll 0.5$) and $log(\chi_r) > 0.5$ (or $\chi_r \gg 3.2$), increasing Δ strongly affect on χ_e.

In Figure 4.12, we plot the relative effective nonlinear coefficient (χ_e/χ_m) against the shape distribution parameter (Δ) for inclusion packing fraction $v_i = 0.08$, and the nonlinear contrast a) $\chi_r = 0.1$, 0.01 and 0.001, and b) $\chi_r = 10$, 100 and 1000. Figure 4.12 a) reveals a monotonically decrease in χ_e/χ_m with increasing Δ. For small Δ, $0 \leq \Delta \leq 0.3$, increasing Δ slightly affects on χ_e/χ_m. Therefore, the small deviation of inclusion shapes from circular cylinder rarely affects on χ_e. However, for large Δ, $0.3 < \Delta \leq 1.0$, χ_e strongly depends on Δ, especially, for high contrast ($\chi_r = 0.001$) and high Δ ($0.6 \leq \Delta \leq 0.1$). Similar behaviors also observed in Figure 4.12 b) but χ_e/χ_m monotonically increase with increasing Δ.

In addition, for $\Delta = 0$, all elliptic cylindrical inclusions are cylinder. The results of χ_e/χ_m agree with those reported in Figure 3.11 for $M = 1$ throughout.

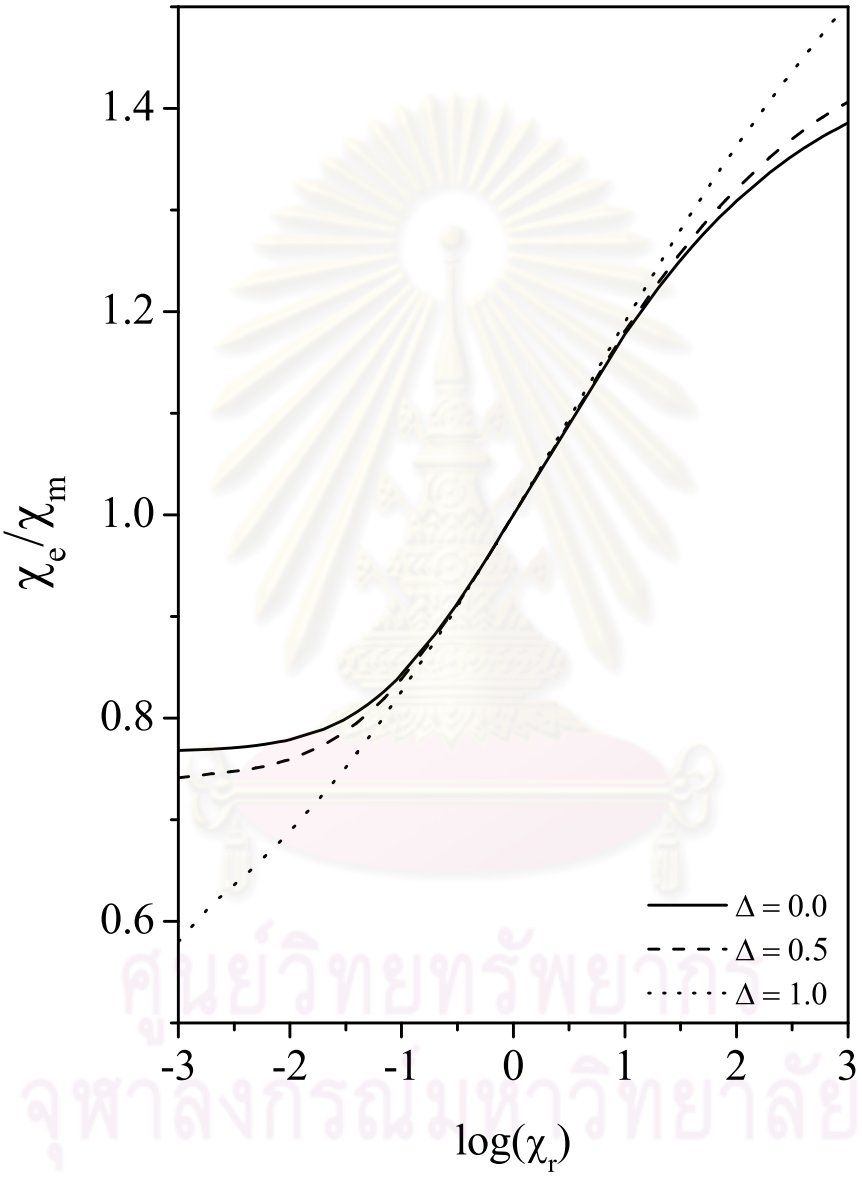

Figure 4.11: The relative effective nonlinear coefficients (χ_e/χ_m) for varying the nonlinear contrast (χ_r) with the shape distribution parameter as parameter.

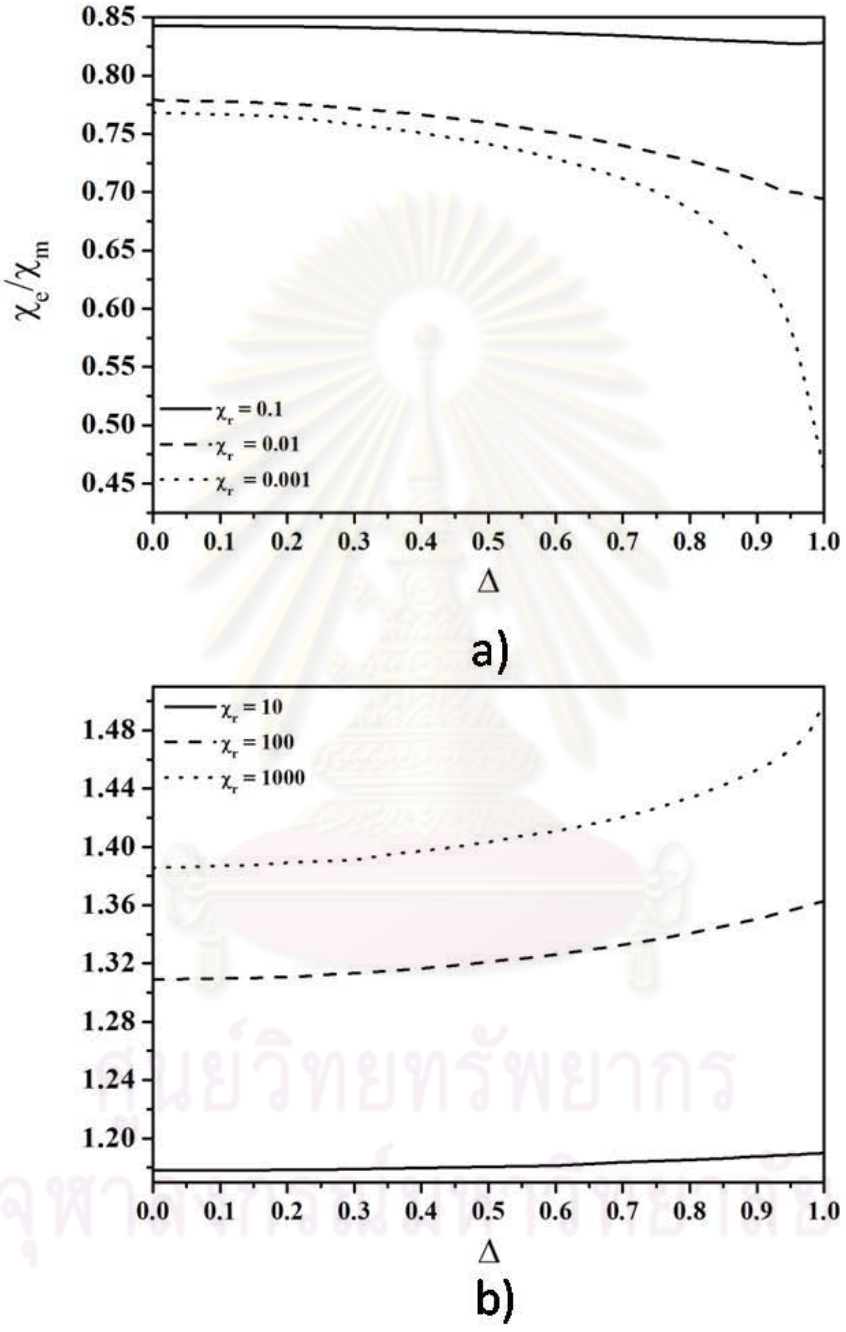

Figure 4.12: The relative effective nonlinear coefficients (χ_e/χ_m) for varying the the shape distribution parameter with the nonlinear contrast (χ_r) as parameter.

CHAPTER V

Conclusions

We have investigated the electric field responses and the effects of inclusion shapes on the effective nonlinear coefficient (χ_e) of weakly and strongly nonlinear elliptic cylindrical dielectric composites. Two types of composites, that with identical inclusion shape and that with distributed inclusion shapes have been considered. For both types, the inclusions are randomly oriented and embedded in the host media. The dielectric property of the inclusions is that the relation between the displacement field ($\mathbf{D}$) and the electric field ($\mathbf{E}$) satisfies a form $\mathbf{D} = \varepsilon\mathbf{E} + \chi|\mathbf{E}|^{\beta}\mathbf{E}$ where β is a nonlinear integer exponent with $\varepsilon \gg \chi|\mathbf{E}|^{\beta}$ for weakly nonlinear composites. For strongly nonlinear composites, the dielectric property of both inclusion and medium satisfying $\mathbf{D} = \chi|\mathbf{E}|^{2}\mathbf{E}$ is considered. Then, the effects of inclusion shapes on the effective nonlinear coefficient (χ_e) are investigated in terms of the aspect ratio (the ratio between the semi-major and semi-minor axes for identical inclusions) and the shape distribution parameter for composites with identical inclusion shape and distributed inclusion shapes, respectively.

Based on the average energy method, the effective nonlinear coefficient (χ_e) relates to the volume average of electric fileds to the power $\beta + 2$ in the inclusion, $\left\langle E_i^{\beta+2} \right\rangle$ and in the host media $\left\langle E_m^{\beta+2} \right\rangle$. These are difficult to obtain. In this research, the determinations on $\left\langle E_i^{\beta+2} \right\rangle$ and $\left\langle E_m^{\beta+2} \right\rangle$ are simplified by using the simple decoupling approximation. This approximation allows us to convert the established results on linear composites to nonlinear composites with the same microstructure. Moreover, it also give an approximate results of $\left\langle E_i^{\beta+2} \right\rangle \approx \left\langle E_i^{2} \right\rangle^{(\beta+2)/2}$ and $\left\langle E_m^{\beta+2} \right\rangle \approx \left\langle E_m^{2} \right\rangle^{(\beta+2)/2}$.

In the first type of composites with identical inclusion shape, we firstly consider a linear composite which consists of linear elliptic cylindrical inclusions with identical shape, having the same aspect ratio, the ratio between major and minor axes (M), randomly oriented and embedded in a different linear dielectric medium in dilute limit. The linear coefficients of inclusions and medium are ε_i and ε_m, respectively. The electric filed inside the elliptic cylindrical inclusions ($\mathbf{E}_i$) is derived by using the elliptic cylindrical coordinates and then applied to determine the effective linear coefficient (ε_e) based on the average field method. The effective linear coefficient (ε_e) is reported in terms of the aspect ratio (M), which the effects of inclusion shapes on ε_e is predicted and reported in section 3.1.4.

Secondly, we consider a weakly nonlinear composites with the same microstructure as in the linear composites which inclusions are randomly oriented and embedded in the linear medium. By using the simple decoupling approximation, the effective nonlinear coefficients (χ_e) of the weakly nonlinear elliptic cylindrical composite are determined for the nonlinear integer exponents (β) equal to 2, 4 and 6. In order to confirm our results of χ_e, we also determine χ_e by using the improved decoupling approximation and the direct method. These give the same results of χ_e because the electric field in the inclusions is uniform. The results of χ_e and the effects of inclusion shapes on χ_e are reported in section 3.2.3.

Thirdly, we focus on strongly nonlinear composites with the same microstructure as the linear composites. The effective nonlinear coefficients (χ_e) are determined by using the simple decoupling approximation. These results on χ_e when the aspect ratio equals 1 agree well with those of Gu and Yu [8], and also confirm the work of Gao and Li [38]. The effects of inclusion shapes on χ_e is reported in section 3.3.3.

In the second type of composites with distributed inclusion shapes, we further consider the composites which have the same microstructure and same dielectric property as described for composites with identical inclusion shape but now the inclusions have variation in shapes. The electric filed inside the elliptic cylindrical inclusions is derived in terms of the depolarization factor (L) and

then applied to determine the effective linear coefficient (ε_e) in terms of the shape distribution parameter (Δ) based on the average field method and the statistical approach. The effects of inclusion shapes on ε_e is analyzed and reported in section 4.1.4.

Next, we extend the work to the weakly nonlinear composites with inclusions having variation in shapes randomly embedded in the linear medium. Based on the statistical approach, the effective nonlinear coefficient of composite with distributed inclusion shapes is related to that of the composites with identical inclusion shape and then the effective nonlinear coefficient (χ_e) is determined by using the simple decoupling approximation. The effects of inclusion shapes on χ_e is investigated and reported in section 4.2.3.

Finally, we concentrate on strongly nonlinear composites with the same microstructure as the linear composites with distributed inclusion shapes. The different approach as that reported for linear composites in section 4.1.2, is employed to determine the effective linear coefficient (ε_e). However, agreement between the two approach is observed, this confirm our work. By using the simple decoupling approximation, the effective nonlinear coefficient (χ_e) is determined and the effects of inclusion shapes on χ_e is discussed and reported in section 4.3.3.

This work provide fundamental information for evaluating the electric field response of weakly nonlinear elliptical dielectric composite, and also for designing nonlinear optical materials for applications in photonic devices or optoelectronic technologies.

In fact, the effective responses of nonlinear composites in external AC electric field has received much attention for both strongly nonlinear and weakly nonlinear composites. Therefore, the effects of inclusion shapes on electric responses of nonlinear composites in external AC electric field with arbitrary nonlinear integer exponet is suggested for further study.

References

[1] Boyd, R. W. *Nonlinear Optic,* 2^{nd} ed. (USA: Acadamic Press, 1992), p 2.

[2] Natenapit, M. Thongboonrithi, C. and Potisook, C. Ninth-order effective responses of nonlinear composites in external DC and AC electric fields. *Physica B* 403 (2008): 4314-4318.

[3] Gu, G. Q. and Yu, K. W. Effective Conductivity of Nonlinear Composite. *Phys. Rev. B* 46 (1992): 4502-4507.

[4] Yu, K., W. Hui, P. M. and Stroud, D. Effective dielectric response of nonlinear composites *Phys. Rev. B* 47 (1993): 14150-14156.

[5] Castaneda, P. P., deBotton, G. and Li, G. Effective properties of nonlinear inhomogeneous dielectrics *Phys. Rev. B* 46 (1992): 4387-4394.

[6] Yu, K. W. and Gu, G. Q. Variational calculation of strongly nonlinear composites *Phys. Lett. A* 193 (1994): 311-314.

[7] Lee, H. C. and Yu, K. W. Effective medium theory for strongly nonlinear composites: comparison with numerical simulations *Phys. Lett. A* 197 (1995): 341-344.

[8] Yu, K. W. and Gu, G. Q. Effective conductivity of strongly nonlinear composites: variational approach *Phys. Lett. A* 205 (1995): 295-300.

[9] Yu, K. W., Hui, P. M. and Lee, H. C. Decoupling approximation for strongly nonlinear composites *Phys. Lett. A* 210 (1996): 115-120.

[10] Yu, K. W. and Yuen, K. P. Effective response of strongly nonlinea composites: Exact results against approximate methods *Phys. Rev. B* 56 (1997): 10740-10742.

[11] Hui, P. M. and Chung, K. H. Effective nonlinear response in random nonlinear granular materials *Physica A* 231 (1995): 408-416.

[12] Lu, W. G. and Li, Z. Y. An improved decoupling approximation method for nonlinear granular composites *Phys. Lett. A* 241 (1998): 197-201.

[13] Stroud, D. and Wood, V. E. Decoupling approxiamtion for the nonlinear-optical response of composite media *J. Opt. Soc. Am. B* 6 (1989): 778-786.

[14] Thongsee, J. and Natenapit, M. Effective nonlinear coefficients of strongly nonlinear dielectric composites *J. Appl. Phys.* 101 (2007): 024303-1-4.

[15] Gehr, R. J., Fischer, G. L. and Boyd, R. W. Nonlinear-optical response of porous-glass-based composite materials *J. Opt. Soc. Am. B* 14 (1997): 2310-2314.

[16] Kochergin, V., Zaporojtchenko, V., Takele, H., Faupel, F. and Föll, H. Improved effective medium approach: Application to metal nanacomposites *J. Appl. Phys.* 101 (2007): 024302-024307.

[17] Piredda, G., Smith, D. D., Wendling, B. and Boyd, R. W. Nonlinear optical properties of a gold-silica composite with high gold fill fraction and the sign change of its nonlinear absorption coefficient *J. Opt. Soc. Am. B* 25 (2008): 945-950.

[18] Giordano, S. Effective medium theory for dispersions of dieclectric ellipsoids *J. Electrostat* 58 (2003): 59-76.

[19] Giordano, S. and Rocchia, W. Shape-dependent effects of dielectrically nonlinear inclusions in heterogenous media *J. Appl. Phys.* 98 (2005): 104101-1-9.

[20] Chang, Q. Ye, H. and Song, Y. Effect of host and particle shape on the optical nonlinearities of nanocomposites *Colloid Surface A* 298 (2007): 58-62.

[21] Natenapit, M. and Thongsri, J. Shape effect on strongly nonlinear response of elliptical composites *Eur. Phys. J. Appl. Phys.* 46 (2009): 20701-1-5.

[22] Goncharenko, A. V., Venger, E. F. and Zavadskii, S. N. Effective absorption cross section of an assembly of small ellipsoidal particles *J. Opt. Soc. Am. B* 13 (1996): 2392-2395.

[23] Goncharenko, A. V., Semanov, Y. G. and Venger, E. F. Effective scattering cross section of an assembly of small ellipsoidal particles *J. Opt. Soc. Am. A* 16 (1999): 517-522.

[24] Gao, L., Yu, K. W., Li, Z. Y. and Hu, B. Effective nonlinear optical properties of metal-dielectric composite media with shape distribution *Phys. Rev. E* 64 (1997): 036615-1-8.

[25] Gao, L. and Huang, Y. Effective nonlinear optical properties of shape distributed composite media *Eur. Phys. J. B* 33 (2003): 165-171.

[26] Gao, L. Effective medium approximation for weakly nonlinear metal/dielectric composite with shape distribution *Phys. Lett. A* 309 (2003): 407-414.

[27] Gao, L., Huang, Y. and Li, Z. Y. Effective medium approximation for strongly nonlinear composite media with shape distribution *Phys. Lett. A* 306 (2003): 337-343.

[28] Gao, L. Maxwell-Garnett type approximation for nonlinear composites with shape distribution *Phys. Lett. A* 309 (2003): 435-442.

[29] Xu, P. and Li, Z. Y. Effect of particle shape on the effective to the percolation threshold *Physica B* 348 (2004): 101-107.

[30] Goncharenko, A. V., popelnukh, V. V. and Venger, E. F. Effect of weak non sphericity on linear and nonlinear optical properties of small particle composites *J. Phys. D: Appl. Phys.* 35 (2002): 1833-1838.

[31] Goncharenko, A. V. Optical properties of core-shell particle composites. I. Linear response *Chem. Phys. Lett.* 386 (2004): 25-31.

[32] Goncharenko, A. V. and Chang, Y. C. Optical properties of core-shell particle composites. II. Nonlinear response *Chem. Phys. Lett.* 439 (2007): 121-126.

[33] Griffiths, D. J. *Introduction to Electrodynamics*, 3^{rd} ed. (USA: Prentice Hall International, 1999), p 135.

[34] Bottcher, C. J. F. *Theory of Electric Polarization*, 2^{rd} ed. vol. 1. (Amsterdam: Elsevier Scientific Publishing Company, 1973), p 100.

[35] Wei, E. B., Gu, G. Q. and Poon, Y. M. Effective properties of graded elliptical cylindrical composites *Physica B* 392, (2007): 327-331.

[36] Stroud, D. and Hui, P. M. Nonlinear susceptibilities of granular matter *Phys. Rev. B* 37 (1988): 8719-8724.

[37] Kraus, J. D. *Electromagnetics*, 4^{rd} ed., (USA: McGraw-Hill International, 1991), p 123.

[38] Gao, L. and Li, Z. Effective response of a strongly nonlinear composite: comparison with variational approach *Phys. Lett. A* 222 (1996): 207-211.

[39] Stratton, J. A. *Electromagnetic Theory,* (London: McGraw-Hill, 1941), p 230.

[40] Landau, L. D. and Lifshitz, E. M. *Electrodynamics of Continuous Medium,* (Oxford: Pergamon, 1984).

[41] Zakri, T., Laurent, J. P. and Vauclin, M. Theoretical evidence for "Lichtenecker's mixture formulae" based on effective medium theory *J. Phys. D: Appl. Phys.* 31 (1998): 1589-1594.

[42] Gao, L., Wan, J. T. K., Yu, K. W. and Li, Z. Y. Effects of highly conducting interface and particle size distribution on optical nonlinearity in granular composites *J. Appl. Phys.* 88 (2000): 1893-1899.

[43] Spiegel, M. R. and Lue, J. *Mathematical handbook of formulas and tables*, 2^{nd} ed., (USA: Schaum's outline series, 1999), p 127.

[44] Thongsri, J. "Effective Nonlinear Coefficient of Strongly Nonlinear Spherical Dielectric Composites,"(Master's Thesis, Department of Physics, Graduate School, Chulalongkorn University, 2005), p 76.

APPENDICES

Appendix A

Improved Decoupling Approximation

For weakly nonlinear composite with identical inclusion shape in section 3.2.2, we use the more accurate expression $\left\langle E_i^{\beta+2} \right\rangle$ to determine the effective nonlinear coefficient (χ_e). For better understanding, in this Appendix, we have to show the process of derivation $\left\langle E_i^{\beta+2} \right\rangle$ in terms of $\langle E_i^2 \rangle$ and $\langle E_i \rangle$.

A.1 Derivation of $\langle E_i^5 \rangle$

In order to improve the results of χ_e, Lu and Li [12] proposed a new decoupling approximation to express $\langle E_i^n \rangle$. When n is odd and $n \geq 3$, it requires

$$\langle (E_i - \langle E_i \rangle)^n \rangle = 0, \tag{A.1}$$

and also n is even;

$$\langle (E_i - \langle E_i \rangle)^n \rangle \approx \left\langle (E_i - \langle E_i \rangle)^2 \right\rangle^{n/2}. \tag{A.2}$$

For $n = 3$, it can be proved that

$$\left\langle E_i^3 \right\rangle = 3 \left\langle E_i^2 \right\rangle \langle E_i \rangle - 2 \langle E_i \rangle^3, \tag{A.3}$$

and also for $n = 4$

$$\left\langle E_i^4 \right\rangle \approx 4 \left\langle E_i^2 \right\rangle \langle E_i \rangle^2 - 4 \langle E_i \rangle^4 + \left\langle E_i^2 \right\rangle^2. \tag{A.4}$$

For more n, by using Eq. (A.1) with $n = 5$, we have to calculate $\langle E_i^5 \rangle$ and obtain

$$\begin{aligned}
&\langle (E_i - \langle E_i \rangle)^5 \rangle = 0 \\
&\left\langle E_i^5 - 5E_i^4 \langle E_i \rangle + 10E_i^3 \langle E_i \rangle^2 - 10E_i^2 \langle E_i \rangle^3 + 5E_i \langle E_i \rangle^4 - \langle E_i \rangle^5 \right\rangle = 0 \\
&\langle E_i \rangle^5 - 5 \langle E_i^4 \rangle \langle E_i \rangle + 10 \langle E_i^3 \rangle \langle E_i \rangle^2 - 10 \langle E_i^2 \rangle \langle E_i \rangle^3 + 5 \langle E_i \rangle \langle E_i \rangle^4 - \langle E_i \rangle^5 = 0 \\
&\langle E_i \rangle^5 = 5 \langle E_i^4 \rangle \langle E_i \rangle - 10 \langle E_i^3 \rangle \langle E_i \rangle^2 + 10 \langle E_i^2 \rangle \langle E_i \rangle^3 - 5 \langle E_i \rangle \langle E_i \rangle^4 + \langle E_i \rangle^5 .
\end{aligned} \tag{A.5}$$

Substituting $\langle E_i^3 \rangle$ and $\langle E_i^4 \rangle$ from Eqs. (A.3) - (A.4) into (A.5), we get $\langle E_i^5 \rangle$ as proposed in Eq. (3.36)

$$\langle E_i \rangle^5 \approx 5 \left\langle E_i^2 \right\rangle^2 \langle E_i \rangle - 4 \langle E_i \rangle^5 . \tag{A.6}$$

A.2 Derivation of $\langle E_i^6 \rangle$

For $n = 6$, the left hand side (L.H.S) of Eq. (A.2) gives

$$\begin{aligned} \langle (E_i - \langle E_i \rangle)^6 \rangle &= \langle E_i^6 - 6E_i^5 \langle E_i \rangle + 15E_i^4 \langle E_i \rangle^2 - 20E_i^3 \langle E_i \rangle^3 + 15E_i^2 \langle E_i \rangle^4 \\ &\quad -6E_i \langle E_i \rangle^5 + \langle E_i \rangle^6 \rangle \\ &= \langle E_i^6 \rangle - 6 \langle E_i^5 \rangle \langle E_i \rangle + 15 \langle E_i^4 \rangle \langle E_i \rangle^2 - 20 \langle E_i^3 \rangle \langle E_i \rangle^3 + 15 \langle E_i^2 \rangle \langle E_i \rangle^4 \\ &\quad -6 \langle E_i \rangle \langle E_i \rangle^5 + \langle E_i \rangle^6 . \end{aligned} \tag{A.7}$$

Replacing $\langle E_i^3 \rangle$, $\langle E_i^4 \rangle$ and $\langle E_i^6 \rangle$ from Eqs. (A.3), (A.4) and (A.6) into (A.7), we obtain

$$\left\langle (E_i - \langle E_i \rangle)^6 \right\rangle = \left\langle E_i^6 \right\rangle - 15 \left\langle E_i^2 \right\rangle^2 \langle E_i \rangle^2 + 15 \left\langle E_i^2 \right\rangle \langle E_i \rangle^4 - \langle E_i \rangle^6 . \tag{A.8}$$

The right hand side (R.H.S) of Eq. (A.2) leads to

$$\begin{aligned} \langle (E_i - \langle E_i \rangle)^2 \rangle^{6/2} &= \left\langle E^2 - 2E \langle E \rangle + \langle E \rangle^2 \right\rangle^3 \\ &= \left(\langle E^2 \rangle - 2 \langle E \rangle \langle E \rangle + \langle E \rangle^2 \right)^3 \\ \langle (E_i - \langle E_i \rangle)^2 \rangle^3 &= \langle E^2 \rangle^3 - 3 \langle E^2 \rangle^2 \langle E \rangle^2 + 3 \langle E^2 \rangle \langle E \rangle^4 - \langle E \rangle^6 . \end{aligned} \tag{A.9}$$

From Eqs. (A.8) - (A.9), we rearrange $\langle E_i^6 \rangle$ and get the expression of $\langle E_i^6 \rangle$ as given in Eq. (3.37) by

$$\left\langle E_i^6 \right\rangle \approx 12 \left\langle E_i^2 \right\rangle^2 \langle E_i \rangle^2 - 12 \left\langle E_i^2 \right\rangle \langle E_i \rangle^4 + \left\langle E_i^2 \right\rangle^3 . \tag{A.10}$$

A.3 Derivation of $\langle E_i^7 \rangle$

We take $n = 7$ to Eq. (A.1) and get

$$\begin{aligned} \langle (E_i - \langle E_i \rangle)^7 \rangle &= 0 \\ &= \langle E_i^7 - 7E_i^6 \langle E_i \rangle + 21E_i^5 \langle E_i \rangle^2 - 35E_i^4 \langle E_i \rangle^3 + 35E_i^3 \langle E_i \rangle^4 - 21E_i^2 \langle E_i \rangle^5 \\ &\quad +7E_i \langle E_i \rangle^6 - \langle E_i \rangle^7 \rangle \\ 0 &= \langle E_i^7 \rangle - 7 \langle E_i^6 \rangle \langle E_i \rangle + 21 \langle E_i^5 \rangle \langle E_i \rangle^2 - 35 \langle E_i^4 \rangle \langle E_i \rangle^3 + 35 \langle E_i^3 \rangle \langle E_i \rangle^4 \\ &\quad -21 \langle E_i^2 \rangle \langle E_i \rangle^5 + 7 \langle E_i \rangle \langle E_i \rangle^6 - \langle E_i \rangle^7 . \end{aligned} \tag{A.11}$$

Eqs. (A.3), (A.4), (A.6) and (A.10) are substituted into Eq. (A.11); therefore, $\langle E_i^7 \rangle$ can be written as given in Eq. (3.38) by

$$\left\langle E_i^7 \right\rangle \approx 14 \left\langle E_i^2 \right\rangle^2 \langle E_i \rangle^3 - 28 \left\langle E_i^2 \right\rangle \langle E_i \rangle^5 + 7 \left\langle E_i^2 \right\rangle^3 \langle E_i \rangle + 8 \langle E_i \rangle^7 . \tag{A.12}$$

A.4 Derivation of $\langle E_i^8 \rangle$

For $n = 8$, L.H.S of Eq. (A.2) leads to

$$\begin{aligned} \langle (E_i - \langle E_i \rangle)^8 \rangle &= \langle E_i^8 - 8E_i^7 \langle E_i \rangle + 28E_i^6 \langle E_i \rangle^2 - 56E_i^5 \langle E_i \rangle^3 + 70E_i^4 \langle E_i \rangle^4 - 56E_i^3 \langle E_i \rangle^5 \\ &\quad +28E_i^2 \langle E_i \rangle^6 - 8E_i \langle E_i \rangle^7 + \langle E_i \rangle^8 \rangle \\ &= \langle E_i^8 \rangle - 8 \langle E_i^7 \rangle \langle E_i \rangle + 28 \langle E_i^6 \rangle \langle E_i \rangle^2 - 56 \langle E_i^5 \rangle \langle E_i \rangle^3 + 70 \langle E_i^4 \rangle \langle E_i \rangle^4 \\ &\quad -56 \langle E_i^3 \rangle \langle E_i \rangle^5 + 28 \langle E_i^2 \rangle \langle E_i \rangle^6 - 8 \langle E_i \rangle \langle E_i \rangle^7 + \langle E_i \rangle^8 . \end{aligned} \tag{A.13}$$

We substitute Eqs. (A.3), (A.4), (A.6), (A.10) and (A.12);

$$\left\langle (E_i - \langle E_i \rangle)^8 \right\rangle = \left\langle E_i^8 \right\rangle + 14 \left\langle E_i^2 \right\rangle^2 \langle E_i \rangle^4 + 28 \left\langle E_i^2 \right\rangle \langle E_i \rangle^6 - 28 \left\langle E_i^2 \right\rangle^3 \langle E_i \rangle^2 - 15 \langle E_i \rangle^8 . \tag{A.14}$$

For the R.H.S of Eq. (A.2), we also obtain

$$\begin{aligned} \langle (E_i - \langle E_i \rangle)^2 \rangle^{8/2} &= \left\langle E_i^2 + 2E_i \langle E_i \rangle + \langle E_i \rangle^2 \right\rangle^4 \\ &= \left(\langle E_i^2 \rangle + 2 \langle E_i \rangle \langle E_i \rangle + \langle E_i \rangle^2 \right)^4 \\ \langle (E_i - \langle E_i \rangle)^2 \rangle^4 &= \langle E_i^2 \rangle^4 - 4 \langle E_i^2 \rangle^3 \langle E_i \rangle^2 + 6 \langle E_i^2 \rangle^2 \langle E_i \rangle^4 - 4 \langle E_i^2 \rangle \langle E_i \rangle^6 + \langle E_i \rangle^8 . \end{aligned} \tag{A.15}$$

Eqs. (A.14) and (A.15) are solved for $\langle E_i^8 \rangle$ given in Eq. (3.39) by

$$\left\langle E_i^8 \right\rangle \approx 24 \left\langle E_i^2 \right\rangle^3 \langle E_i \rangle^2 - 8 \left\langle E_i^2 \right\rangle^2 \langle E_i \rangle^4 - 32 \left\langle E_i^2 \right\rangle \langle E_i \rangle^6 + 16 \langle E_i \rangle^8 + \left\langle E_i^2 \right\rangle^4 . \tag{A.16}$$

Appendix B

Experiences

National Presentations:

2005 J. Thongsee and M. Natenapit. Effective Nonlinear Coefficients of Strongly Nonlinear Cylindrical Dielectric Composites by Decoupling Technique. *Siam Physics Congress 2008*, Khao Yai, Nakorn Ratchasima, Chiangmai, Thailand (20-22 March 2008): PB 14

2009 J. Thongsri and M. Natenapit. Effective Nonlinear Response of Weakly Nonlinear Ellipticall Dielectric Composites. *Siam Physics Congress 2009*, Cha-am, Petchaburi, Thailand (19-21 March 2009): CT-07.

Teacher Assistant:

Jun 2003 - Mar 2009	General Physics Laboratory I-II
Jun 2006 - Sep 2006	Electricity and Magnetism I
Nov 2006 - Mar 2007	Mathematical Method for Physics II
Jun 2007 - Sep 2007	Statistical Physics I
Nov 2007 - Mar 2008	Mathematical Method for Physics I
Jun 2008 - Sep 2008	General Physics I
Nov 2008 - Mar 2009	General Physics II

Vitae

Mr. Jatuporn Thongsri was born on January 10, 1979 in Surin province, Thailand. He has obtained a scholarship from the Development and Promotion of Science and Technology Talent Project (DPST) since 1995. He graduated with the Bachelor Degree of Science in Physics from Khonkaen University in 2001 and with the Master Degree in the same field from Chulalongkorn University in 2005.

Publications:

2007 J. Thongsee and M. Natenapit. Effective nonlinear coefficients of strongly nonlinear dielectric composites *J. Appl. Phys.* **101** (2007): 024303-1-4.

2009 M. Natenapit and J. Thongsri. Shape Effect on Strongly Nonlinear Response of Elliptical Composites *Eur. Phys. J. Appl. Phys.* **46** (2009): 20701-1-5.

2011 J. Thongsri and M. Natenapit. Shape Effect on Weakly Nonlinear Elliptical Composites *(to be published).*

International Presentations:

2008 J. Thongsee and M. Natenapit. Effective Response of Nonlinear Elliptical Dielectric Composites 4^{th} *Mathematics and Physical Sciences Graduate Congress, National University of Singapore*, Singapore (17-19 December 2008): PB 01 (Chairman).

2009 J. Thongsri and M. Natenapit. Effective Nonlinear Coefficients of Weakly Nonlinear Elliptical Dielectric Composites 5^{th} *Mathematics and Physical Sciences Graduate Congress, Chulalongkorn University*, Bangkok, Thailand (7-9 December 2009): PM 517.